

Lawrence Berkeley National Laboratory

Recent Work

Title

CALORIMETRIC DETERMINATION OF THE TRANSITION ENERGY OF URANIUM-235m

Permalink

<https://escholarship.org/uc/item/2sr748gh>

Author

Culler, Barbara Ellen Bailey.

Publication Date

1971-08-01

LBL-221

c.2

DOCUMENTS SECTION

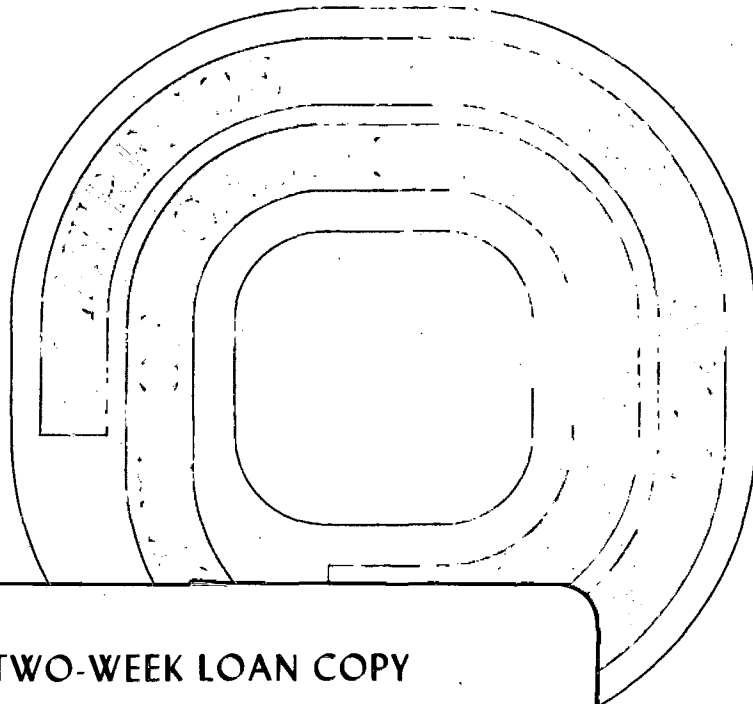
DOCUMENTS SECTION

CALORIMETRIC DETERMINATION OF THE
TRANSITION ENERGY OF URANIUM-235m

Barbara Ellen Bailey Culler
(Ph. D. Thesis)

August 1971

AEC Contract No. W-7405-eng-48



TWO-WEEK LOAN COPY

*This is a Library Circulating Copy
which may be borrowed for two weeks.
For a personal retention copy, call
Tech. Info. Division, Ext. 5545*

LBL-221

c.2

4

DISCLAIMER

This document was prepared as an account of work sponsored by the United States Government. While this document is believed to contain correct information, neither the United States Government nor any agency thereof, nor the Regents of the University of California, nor any of their employees, makes any warranty, express or implied, or assumes any legal responsibility for the accuracy, completeness, or usefulness of any information, apparatus, product, or process disclosed, or represents that its use would not infringe privately owned rights. Reference herein to any specific commercial product, process, or service by its trade name, trademark, manufacturer, or otherwise, does not necessarily constitute or imply its endorsement, recommendation, or favoring by the United States Government or any agency thereof, or the Regents of the University of California. The views and opinions of authors expressed herein do not necessarily state or reflect those of the United States Government or any agency thereof or the Regents of the University of California.

CALORIMETRIC DETERMINATION OF THE TRANSITION ENERGY OF URANIUM-235m

Contents

Abstract vii

I. Introduction 1

II. Calorimeter 5

 A. Introduction 5

 1. Fundamentals of Calorimetry--Unsuitability of
 Conventional Methods for this problem. 5

 2. Wheatstone Bridge Calorimeter. 5

 3. Thermistors. 6

 B. Calorimeter Design 8

 1. Early Designs. 8

 a. A.C. feedback bridge 8

 b. "KQED effect". 8

 2. Final Design and Circuit Diagram 9

 a. Thermistors. 9

 b. Fixed resistors and associated circuitry 18

 c. Photocells and galvanometer. 21

 d. VTVM and recorder. 27

 e. Vacuum system. 27

 f. Constant temperature bath. 28

 C. Operating Procedure. 29

 1. Use of Helium. 30

 2. Heating Phase. 30

 D. Calibration of Calorimeter 32

III. Chemistry. 34

 A. Solvent Extraction 34

1. Theoretical Considerations 34

 a. Introduction 34

 b. Aqueous phase. 35

 c. Organic extractant 37

2. Experimental Extraction Work 39

 a. Choice of salting-out agent. 39

 b. Reducing agent for plutonium 40

 c. Plutonium chemistry. 41

 d. Plutonium peroxide precipitations. 45

 e. Ether-associated peroxides 47

B. Ion Exchange 48

 1. Theoretical Considerations 49

 a. History. 49

 b. Description of resin structure 49

 c. Mechanism of exchange. 50

 2. Experimental Work. 52

 a. Description of materials and procedure 52

 b. Cation exchange. 54

 c. Zeolite. 54

 d. Anion exchange 55

IV. Experimental Procedure 58

 A. Extraction and Other Gloved Box Operations 58

 B. Column 60

 C. Preparation of Sample. 60

 D. Operation of Calorimeter 61

 E. Determination of Yield 63

V. Results and Discussion	66
A. Introduction	66
B. Uranium 235-m Runs	67
C. Bismuth-212 Run.	83
VI. Alpha Half Life Calculation and Cosmological Consequences. .	93
A. Uranium Cosmochronology.	93
B. Coulomb Excitation Calculation	94
C. Calculation of the Half Life for Alpha Decay of ^{235m} U.	98
D. Cosmological Consequences.	104
VII. Summary and Conclusions.	105
Acknowledgments.	107
References	109

CALORIMETRIC DETERMINATION OF THE TRANSITION ENERGY OF URANIUM-235m

Barbara Ellen Bailey Culler

Lawrence Berkeley Laboratory
University of California
Berkeley, California 94720

August 1971

ABSTRACT

The isomeric state of uranium-235 decays by internal conversion, emitting electrons of extremely low energy. Hence, the transition energy is difficult to measure by conventional means. A microcalorimeter was designed and constructed to measure directly the heat produced by the decay. The value obtained for the transition energy was 572 ± 33 eV.

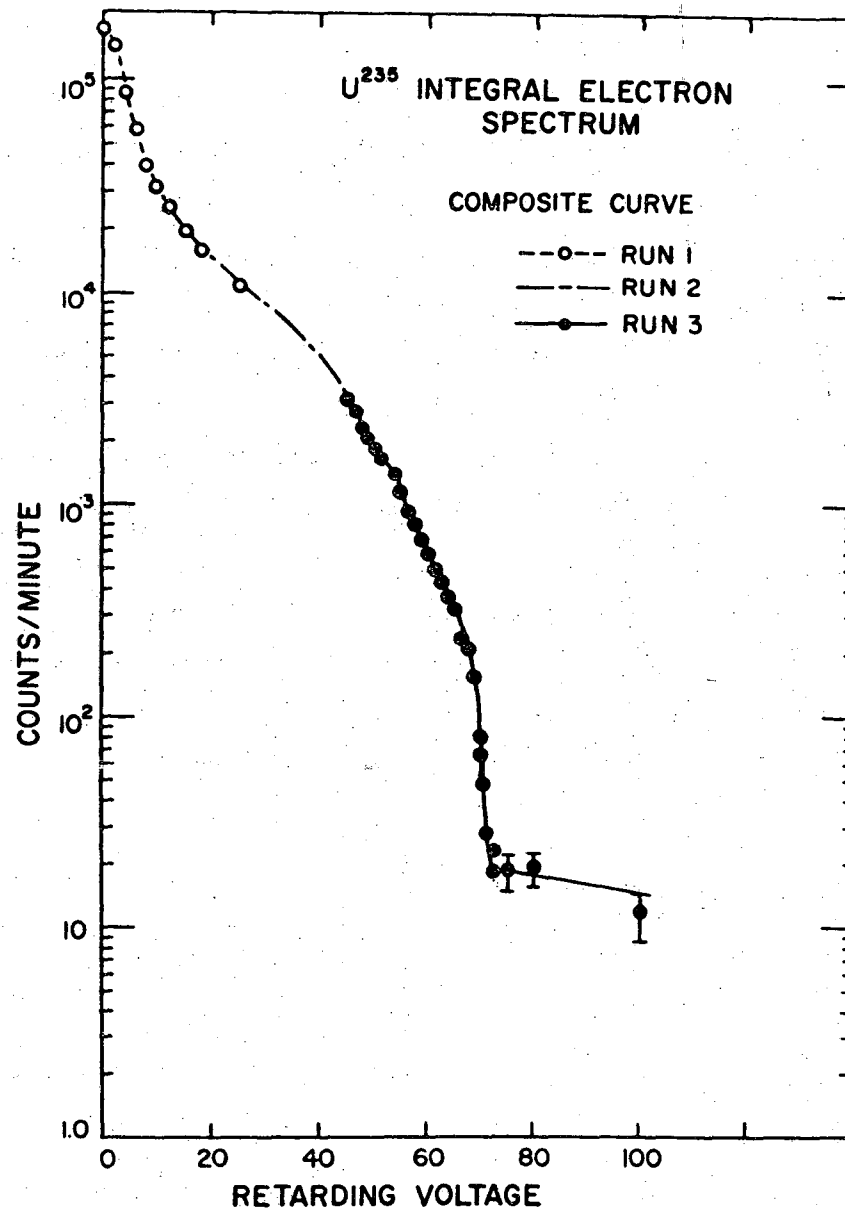
The half life for alpha decay of the isomer was calculated to be 5.9×10^8 years. In addition the probability of Coulomb excitation of the isomeric state by interstellar protons was estimated and found to be negligible. These two results eliminate a possible uranium-235 removal mechanism in space, and substantiate the use of the ratio $^{235}\text{U}/^{238}\text{U}$ to determine the age of the galaxy.

I. INTRODUCTION

For several years a puzzling anomaly appeared to exist in the alpha decay of plutonium-239 to uranium-235. Favored alpha decays of odd-A nuclei such as plutonium-239 populate levels in which the spin of the unpaired nucleon remains unchanged. Since plutonium-239 has a ground state spin of $1/2^+$, one would expect alpha decay to a $1/2^+$ state in uranium-235. However, the ground state of uranium-235 is $7/2^-$, and there is no obvious gamma transition between a $1/2^+$ level and the $7/2^-$ ground state. This suggested that plutonium-239 decayed to an excited state of uranium which had either a very long half life or very low energy. But an E3 transition in an actinide is unlikely to have a long half life. This was confirmed by Huizenga, *et al.*,¹ who compared the optical spectrum of uranium-235 separated from a ten-year old sample of plutonium-239 with that of normal uranium. They were able to set an upper limit of four months on the transition half life.

Shliagin, in 1956,² found 2 keV conversion electrons, and in 1957 Asaro and Perlman³ reported conversion electrons of less than 1 keV with a half life of 26.5 ± 0.2 minutes. Nearly simultaneously, Huizenga *et al.*⁴ determined a half life of 26.6 ± 0.3 minutes for very soft conversion electrons.

Using an integral single-retarding-field electrostatic analyzer, Michel *et al.*⁵ reported the electron spectrum shown in Fig. 1. The source was prepared by collecting recoil nuclides from a thin plutonium-239 deposit. The samples were collected on foils of several different metals, using various negative potentials to deposit the ions which had dissipated their recoil energy in air.



XBL 718-1310

Fig. 1. Integral energy spectrum of soft electrons accompanying isomeric transition of U^{235m}.

The uranium-235m conversion electron energy was also investigated by M. S. Freedman et al.,⁶ using both electrostatic and magnetic spectroscopy. The source preparation, using 8 mg of plutonium-239, was basically similar to that of Michel et al. The upper limit of the transition energy was reported to be 23 eV.

More recently, Mazaki and Shimizu,⁷ also using the electrostatic retarding method on a sample of uranium-235m prepared by recoil collection, obtained a transition energy of 30 ± 3 eV.

Finally, Neve de Mevergnies⁸ has repeated the experiment with a more active source than those used by Freedman et al. and by Mazaki and Shimizu, and has observed a cut-off near 65 eV. Adding the work function of platinum, on which the sample was collected, and the probable electron binding energies, the transition energy is calculated to be 73 ± 5 eV.

Several points should be noted concerning these four results. First, all four depend upon a mass-free source of uranium-235m from which the electrons can escape without serious energy degradation. Since most of the electrons observed in these experiments had energies less than 1 eV, this condition has not been met. Furthermore, Michel et al. noted that the shape of the curve in the medium energy region could be changed slightly by varying the conditions of recoil collection, particularly the surface treatment of the collection foil and the accelerating voltage, a further indication that sample preparation is a crucial factor in the results.

Secondly, the higher end points observed by Michel et al. and de Mevergnies were obtained from much more active sources than those used in the two experiments which resulted in a lower energy, suggesting that

the actual end point of the spectrum perhaps has not been seen in any of these measurements--that electrons of higher energies are simply too few in number to be detected.

This hypothesis could also be inferred from the third point, namely that the spectrum of Michel et al. had several data points of low intensity beyond the 70 eV cut-off. These points were attributed at the time to instrumental noise.

No further refinements in instruments, however, can alleviate the fact that determination of the transition energy of uranium-235m by direct measurement of the electron energy is limited by the inability to obtain in sufficient quantity electrons undegraded in energy.

The very fact that so much of the electron energy is absorbed within the sample suggests a totally different means of measuring the transition energy--calorimetry. Here, the experimental difficulties of the spectroscopic method may be utilized in a positive manner.

II. CALORIMETER

A. Introduction

1. Fundamentals

Calorimetry has been used extensively in the study of nuclear phenomena. It has the advantages of high accuracy, direct interpretation of data and versatility; it is possible to measure activity, half life, disintegration energy or mass of the sample. However, conventional calorimetry is obviously out of the question for the determination of the transition energy of uranium-235m, since the amount of heat produced by the decay of the isomer is so very small. Assuming a transition energy of 70 eV, a sample containing 10^{12} d/min (the expected yield in this experiment) will produce 2.7×10^{-6} cal/min, or 1.9×10^{-7} watt.

An exceptionally sensitive calorimeter is required, one whose heat capacity is kept as low as possible. In the limiting case the heat detector may be made to function as the calorimeter vessel itself.

A Wheatstone bridge calorimeter was chosen for the measurement. In this type of calorimeter one or two arms of the bridge are devices whose resistance changes with temperature; the imbalance of the bridge may then be measured and related to this temperature difference, and if the heat capacity of the system is known or can be calibrated, the total amount of heat produced in the radioactive decay is readily calculated.

2. Wheatstone Bridge Calorimeter

The calorimeter designed for this experiment basically consists of four precision resistors of known value and two thermally dependent resistors arranged in a Wheatstone bridge circuit with a galvanometer

connected across it. A variable precision resistor is placed in parallel with two of the known resistors to compensate for small differences in resistance. Figure 2 illustrates the basic circuit.

When a sample of uranium-235m is placed on one of the heat-sensitive resistors, the self-absorption of the soft electrons within the sample and resistor will change its temperature and therefore the resistance of that arm of the bridge. The bridge must then be rebalanced by the variable resistor. As the activity dies away with its 26.5 minute half life, the resistance of the sample-containing device will change accordingly, and the resulting imbalance of the bridge may be measured as a function of time, and related to the energy dissipated within the sample.

3. Thermistors

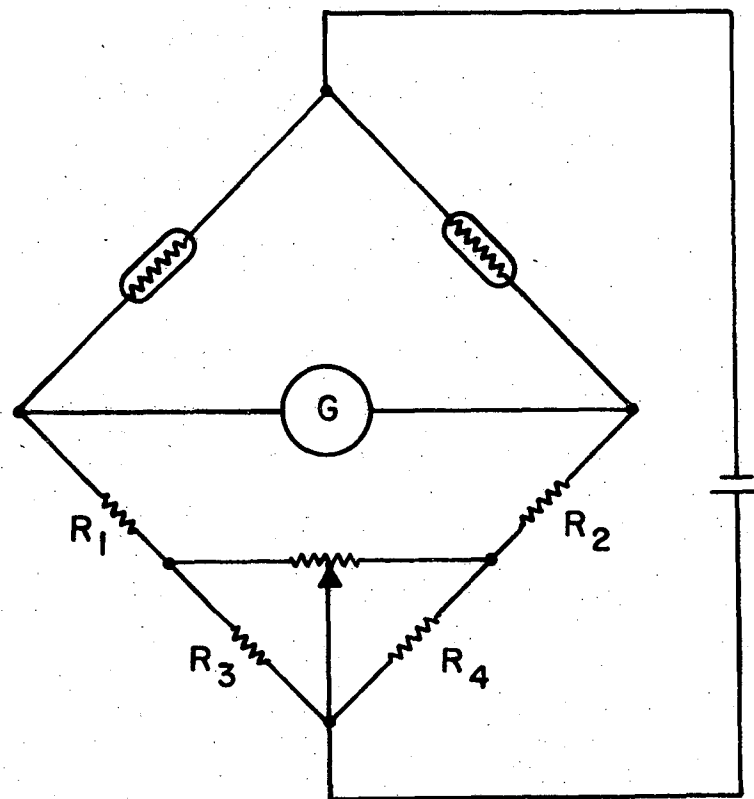
Thermally dependent resistors, or thermistors, are devices which make use of the large temperature coefficient of resistivity of semiconductors. Whereas the resistivity of a metal rises with increasing temperature, a semiconductor has a negative coefficient of resistivity, or a decrease in resistivity with increasing temperature. Moreover, semiconductors are much more sensitive to temperature than metals. For instance, a typical metal, starting from room temperature, will double its resistivity if the temperature rises about 300°C. However, semiconductor materials can be prepared whose resistivities will decrease to half their initial values if the temperature rises only 18°C.⁹

B. Calorimeter Design

1. Early Designs

a. A.C. feedback bridge. A bridge similar to that described in fig. 2 was constructed. R_1 and R_2 were wire-wound resistors of 21.5 K, R_3 and R_4 were wire wound resistors of 2K, and the variable resistor was a 20 K Ω Helipot. The galvanometer was used to detect the imbalance of the bridge due to the decaying uranium-235m and to feed back an appropriate 20 KHz signal to the sample-holding thermistor. In this way the thermistor would be heated sufficiently to compensate exactly for the decaying power output of the sample. The amount of radio frequency power needed to balance the bridge was measured as a function of time. The responses of several different designs of this type were very slow and none too smooth, and all were inadequate for the measurement.

b. "KQED effect". In the course of these tests it became apparent that certain unknown factors were causing a severe instability in the calorimeter, as indicated by a very erratic recorder tracing of power vs. time. It was shown that the problem was related to the temperature sensitivity of the thermistors, since a smooth tracing was obtained if the thermistors were replaced by metal film resistors. Walking near the apparatus when the power to the bridge was turned on produced major deflections. Since static electricity did not affect matters, it seemed likely that radio frequency fields were being picked up by some part of the apparatus and power was being dissipated in one or both thermistors. A sensitive radio receiver coupled to the bridge showed the presence of strong FM and television signals. The local educational television station, at 186 - 192 MHz was strongest and was of the order of 1 mV on



XBL718 - 4041

Fig. 2. Basic circuit for Wheatstone bridge calorimeter.

the left thermistor. The trouble was eliminated by more careful grounding of the double-shielded cables connecting the galvanometer and the thermistors to the rest of the bridge.

2. Final Design and Circuit Diagram

It was decided to make the measurement in a completely different fashion. No attempt was made to keep the bridge balanced, but the mirror-type galvanometer was kept in a null position by allowing the light beam reflected from its mirror to impinge on a cadmium-selenide photocell, which functioned as a variable resistor between the galvanometer and a battery, allowing just enough current to flow through the galvanometer coil to keep the galvanometer beam in a fixed position very near its zero point. The magnitude of this current was proportional to the bridge imbalance, and was recorded as the calorimeter output signal. This system worked very well. The final circuit diagram of the calorimeter is shown in Fig. 3.

a. Thermistors: The arrangement and function of the components of this circuit will now be considered in more detail. In the block marked "1" are the two thermistors.

Thermistors may be made in a variety of sizes, shapes and electrical properties. A very small bead thermistor is required for the Wheatstone bridge calorimeter to minimize the heat capacity of the instrument. The thermistor chosen is described in Fig. 4.

If such a thermistor is placed in an evacuated vessel and is at a temperature higher than ambient, heat will be lost by conduction along the leads, radiation from the bead and leads and by convection.

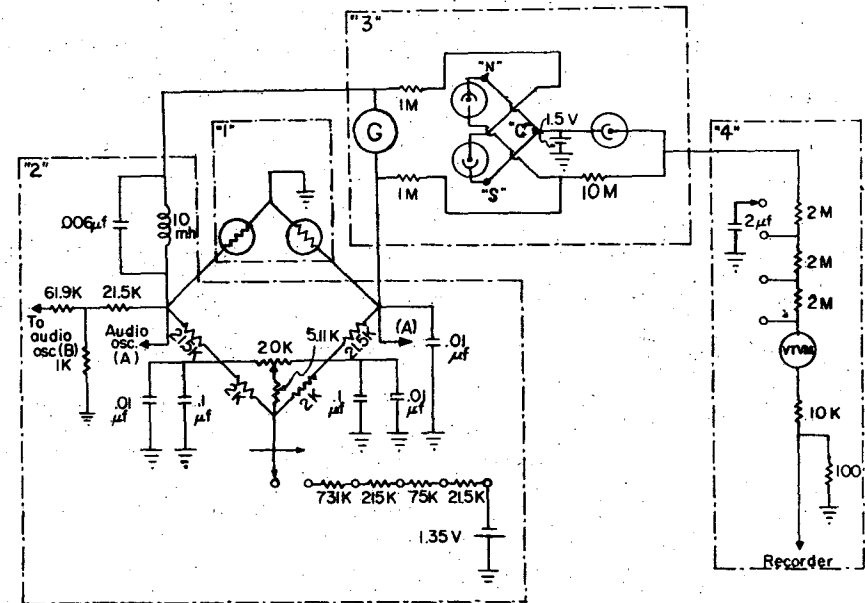
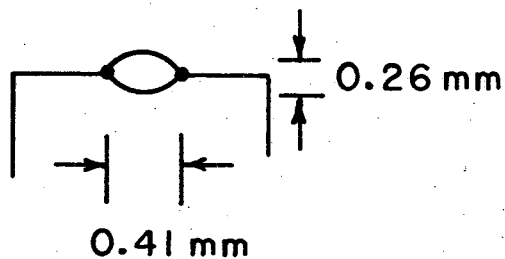


Fig. 3. Circuit diagram of Wheatstone bridge calorimeter.



XBL718-4038

Leads are 0.025 mm platinum-iridium wire, about 1 cm long

density: 2.5 g/cm^3

mass: $3.6 \times 10^{-5} \text{ g}$

heat capacity = $C = 1 \times 10^{-5} \text{ cal/}^\circ\text{C}$

area of bead = $A_b = 3.0 \times 10^{-3} \text{ cm}^2$ (assuming ellipsoidal bead)

cross-sectional area of each lead = $A_l = 4.9 \times 10^{-6} \text{ cm}^2$

Conduction and radiation from the bead predominate. Radiation from the leads is negligible because their surface area is much less than that of the warmer bead. Convection losses are also negligible because the system is evacuated. The total rate of heat loss is thus

$$H_T = H_C + H_R,$$

where H_C is the rate of loss by conduction and H_R is the rate of loss by radiation from the bead.

H_C is given by twice the usual equation, since there are two leads.

$$H_C = 2 K_{Pt} A_l \theta / L,$$

where K_{Pt} = thermal conductivity of platinum-iridium alloy

θ = temperature above ambient in $^\circ\text{C}$

L = length of lead

$$H_C = 4.1 \times 10^{-5} \theta \text{ cal/min} = 2.9 \times 10^{-6} \theta \text{ watt}$$

H_R follows from Stefan's Law and may be expressed:

$$H_R = A_b e \sigma (T_b^4 - T_o^4),$$

where e = emissivity of glass (the bead is glass-coated)

σ = Stefan-Boltzmann constant

T_b = temperature of bead = $T_o + \theta$

T_o = ambient temperature

Fig. 4. Description of thermistor bead, Veco 31A7, Victory Engineering Co.

$$H_R = A_b e \sigma (T_o + \theta)^4 - T_o^4$$

Since $\theta \ll T_o$, terms of second and higher order in θ are negligible in a binomial theorem expansion.

$$H_R = 4A_b e \sigma T_o^3 \theta$$

$$H_R = 2.4 \times 10^{-5} \theta \text{ cal/min} = 1.9 \times 10^{-6} \theta \text{ watt}$$

The combined effects of conduction and radiation losses thus follow Newton's Law of Cooling.

$$H_T = k \theta$$

where

$$\begin{aligned} k &= (4.1 \times 10^{-5}) + (2.4 \times 10^{-5}) = 6.5 \times 10^{-5} \text{ cal/min-}^\circ\text{K} \\ &= 4.6 \times 10^{-6} \text{ watt/}^\circ\text{K} \end{aligned}$$

To find θ , the rise in temperature of the thermistor bead at any time, one must consider the heat being dissipated in the bead by the radioactive decay of the sample and the heat losses from conduction and radiation in the differential equation:

$$\frac{d\theta}{dt} = \frac{\text{rate of heat production}}{C} - \frac{\text{rate of heat loss}}{C}$$

where C = heat capacity of the thermistor. The rate of heat production at any time, t , is given by the initial amount of heat produced by the sample times the fraction of the sample remaining at time t . The rate of heat loss has been derived in the previous calculation. Thus,

$$\frac{d\theta}{dt} = \frac{2.7 \times 10^{-6} e^{-\lambda t}}{C} - \frac{k\theta}{C}$$

The general solution is

$$\theta = \frac{2.7 \times 10^{-6}}{C(\lambda - \frac{k}{C})} (e^{-\frac{k}{C}t} - e^{-\lambda t}) + \theta_o e^{-\frac{k}{C}t}$$

where θ_o is the difference in temperature between the thermistor and ambient at $t = 0$.

$$\theta = -4.15 \times 10^{-2} (e^{-6.5t} - e^{-0.026t}) + \theta_o e^{-6.5t}$$

The first term in this equation for θ describes the effect due to the power dissipated within the thermistor by the radioactive decay of the sample. The second term shows the thermal behavior of the thermistor as a result of an initial temperature difference, θ_o , at $t = 0$.

The response time of the thermistor may be evaluated by calculating the time required for θ_o to decrease by a factor of 10. In the absence of any heat source the first term in the equation for θ is zero. Then,

$$\theta = 10^{-1} \theta_o = \theta_o e^{-6.5t}$$

Solving for t ,

$$t = 0.354 \text{ minutes}$$

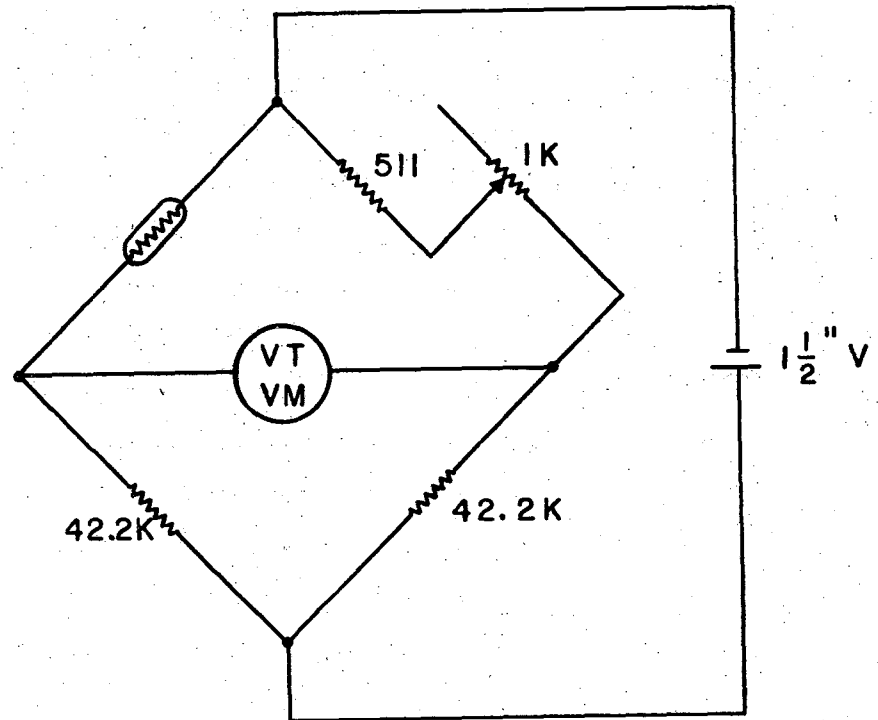
Thus, an initial temperature difference between the thermistor and ambient will decrease a factor of 10^{10} in 3.54 minutes.

An estimate of the maximum temperature rise due to the decay of the sample may be calculated by neglecting the term in θ_0 . Differentiating and setting the resulting equation equal to 0, the maximum temperature rise is found to occur at 0.85 minute and is equal to 0.04°C .

Two Veco 31A7 thermistors were used in the calorimeter circuit as two arms of the bridge--one was the sample holder, the other was a reference thermistor to cancel out temperature effects or any effects due to the semiconductor nature of the sample-holding thermistor.

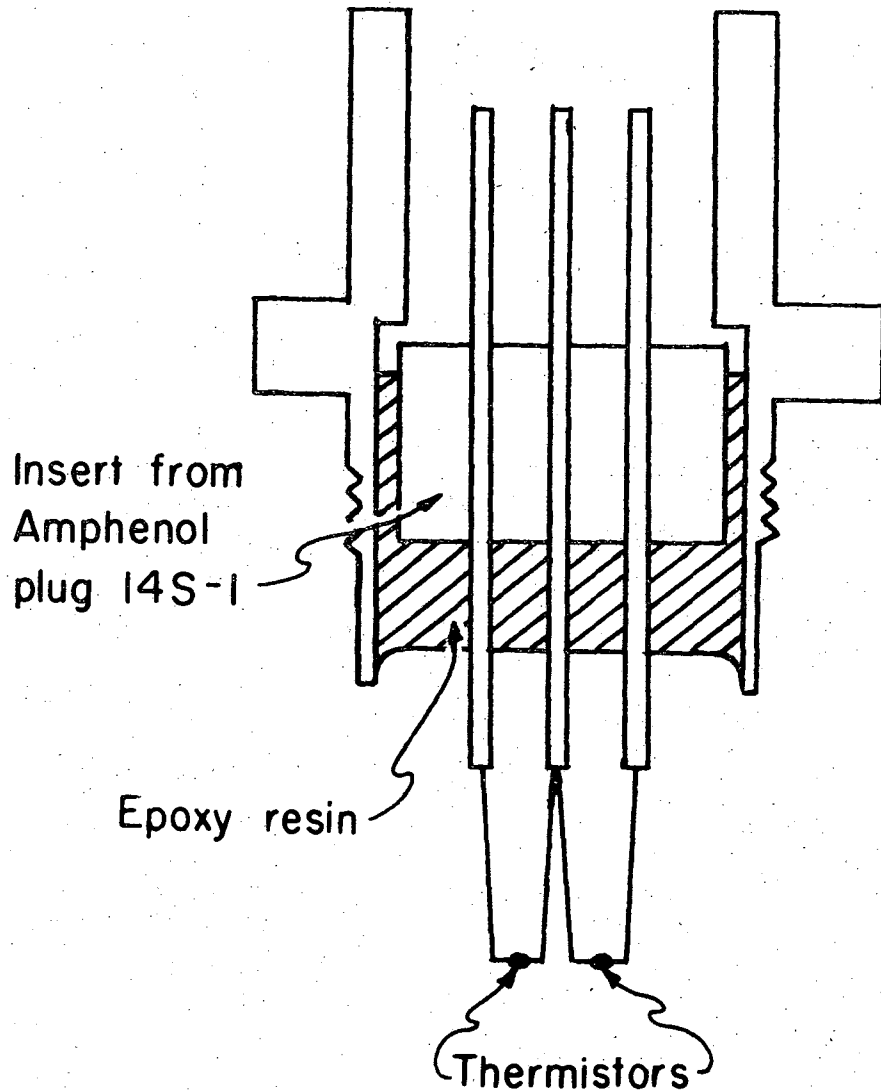
It is desirable to match the two thermistors as closely as possible in resistance to make the bridge more easily balanced. Small differences in resistance may be compensated for by the variable resistor. The resistances of the thermistors were measured at the operating temperature of the calorimeter, and a null method was employed.

The circuit used to measure the resistance of the thermistors is shown in Fig. 5. The resistance of the thermistor is given by 511Ω plus the setting on the variable resistor. Each matched pair of thermistors used in the experiments is mounted in a Dural holder shown in Fig. 6. The interior of an Amphenol 14S-1 connector is centered in the holder so that the three terminals are about $1/4$ inch above the top of the holder and then held in place by epoxy resin. The thermistors are soldered to the terminals with low thermal emf solder. Any thermistor mount can be quickly inserted into the calorimeter circuit by plugging it into a matching connection in the calorimeter vessel. A small aluminum cap screws on over the thermistors (this will be discussed further in Sec. C, Operating Procedure) and a large copper cover screws over this to make a vacuum tight seal with the rest of the calorimeter vessel. An exploded



XBL718-4042

Fig. 5. Circuit for measuring the resistance of thermistors.



XBL 718-1297

Fig. 6. Thermistor holder.

view of the apparatus is shown in Fig. 7. All of the parts except the thermistor holder and the small protective cap were made of copper for optimum heat conductivity. The calorimeter vessel is immersed about six inches in a constant temperature water bath which will be discussed in Sec. B2. The insulated leads from the thermistors were cemented to the side of the eight-inch long vacuum connection and soldered to pins that protrude through a brass plug at the top. This plug and the terminals are made vacuum tight by a layer of Apiezon-W vacuum wax.

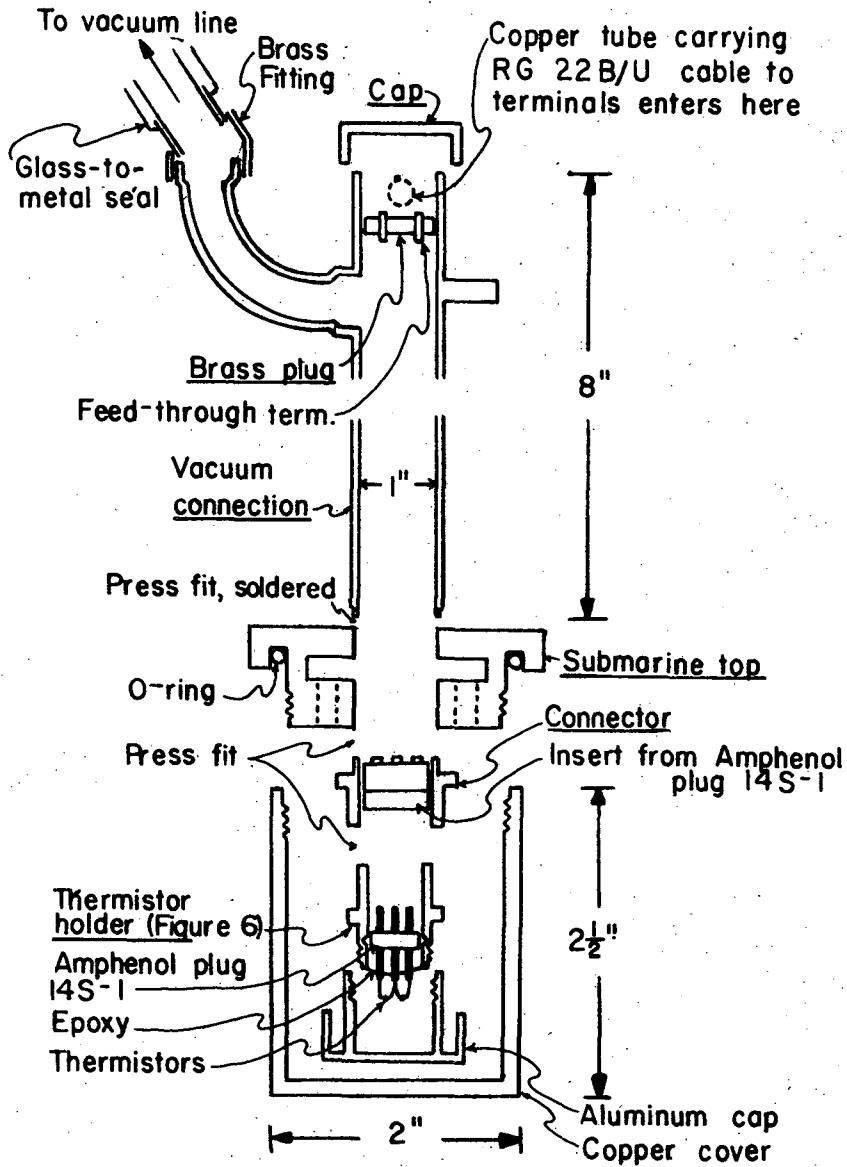
The signal from the thermistors is brought from the terminals in the plug of the calorimeter vessel to the rest of the bridge circuit by a two-foot length of doubly-shielded twin lead cable, Amphenol RG 22 B/U.

b. Fixed resistors and associated circuitry. Block 2 represents a brass tank in which is arranged the remainder of the bridge circuitry. The tank is also immersed in the constant temperature bath. Four shelves inside the tank hold the various components, as shown in Fig. 8.

There are refinements on the basic bridge circuit of Fig. 2, which will be considered individually.

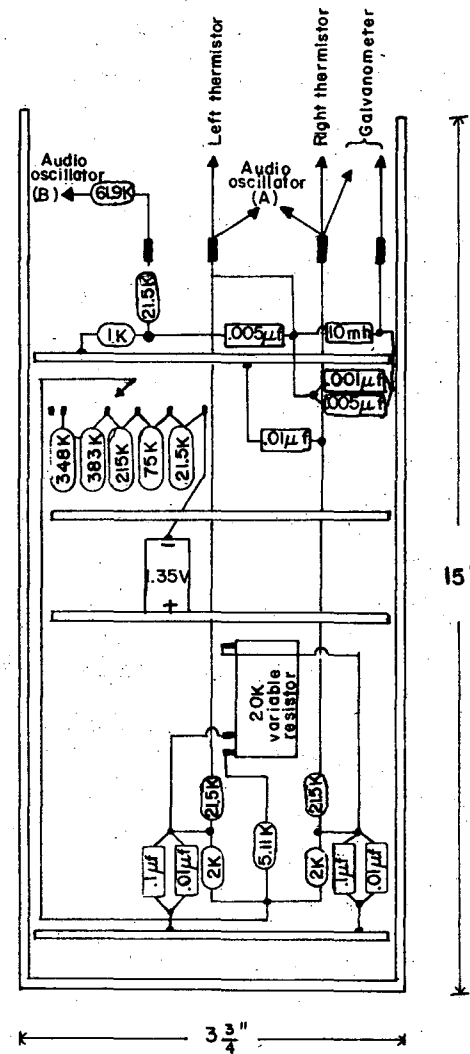
The battery is equipped with a switch which allows the bridge to operate at 1/100, 1/30, 1/10, 1/3 or full voltage for different degrees of sensitivity.

There is a 2K resistor in series with each fixed resistor of 21.5K, with the end points of the 20K variable resistor attached between them. These serve to reduce the sensitivity of the 20K variable resistor so that fine adjustments in the bridge balance may be made more easily. The 0.1 and 0.01 μ f capacitors going to ground from this junction bypass any A.C. voltage which may be present.



XBL 718-4083

Fig. 7. Exploded view of calorimeter.



XBL 718-4082

Fig. 8. Brass resistor tank.

The points labeled "audio osc. (A)" are points at which a 20 KHz signal from an audio oscillator (Hewlett-Packard model 200 AB) may be applied to the thermistors. This will be discussed in more detail in Sec. C, Operating Procedure. The point marked "audio osc. (B)" is where a 20 KHz signal is applied to the left thermistor for calibration purposes. The choke prevents any of these 20 KHz signals from affecting the galvanometer.

c. Photocells and galvanometer. Block 3 is located in a darkroom because it contains the light-sensitive portions of the circuit, namely three cadmium selenide photocells--Clairex type CL 3. These are arranged in series with a 1.35 V mercury cell and the mirror type galvanometer, and function as variable resistors which govern the amount of current reaching the galvanometer. The central photocell is three meters from the galvanometer mirror and in such a position that the beam from the mirror must drift past it to reach its zero point. An imbalance in the calorimeter bridge will also cause the beam from the galvanometer to move, of course. As the beam impinges on the photocell, its resistance drops from about 100MΩ to a value which depends upon the intensity of the light beam and the area of the photocell which is in the light beam, thereby allowing current from the 1.35 V cell to flow through the galvanometer coil and deflect it in the opposite direction. This current is thus a function of the imbalance of the bridge, and may be measured accurately as a function of time. Since the intensity of the beam must be as nearly constant as possible, the light source is supplied by a constant voltage regulator, Sorensen

type 1000S. A variable transformer controls the actual level of the light.

The other two photocells are positioned one on each side of the galvanometer beam about halfway between the central photocell and the galvanometer. They are convenient centering devices which prevent the galvanometer beam from swinging too far from the central photocell. The points marked "N" and "S" are terminals, either of which may be shorted to the central terminal "C" by the fingers in order to deflect the galvanometer beam one way or the other, thus permitting quick manual centering of the beam.

In order to determine the sensitivity of the calorimeter with a given galvanometer, consider the bridge circuit shown in Fig. 9 with the currents as labeled. The resistances labeled R_1 are the large fixed resistances, R_r is the reference thermistor resistance, R is the sample-holding thermistor resistance, R_g is the resistance of the galvanometer, and E is the applied voltage.

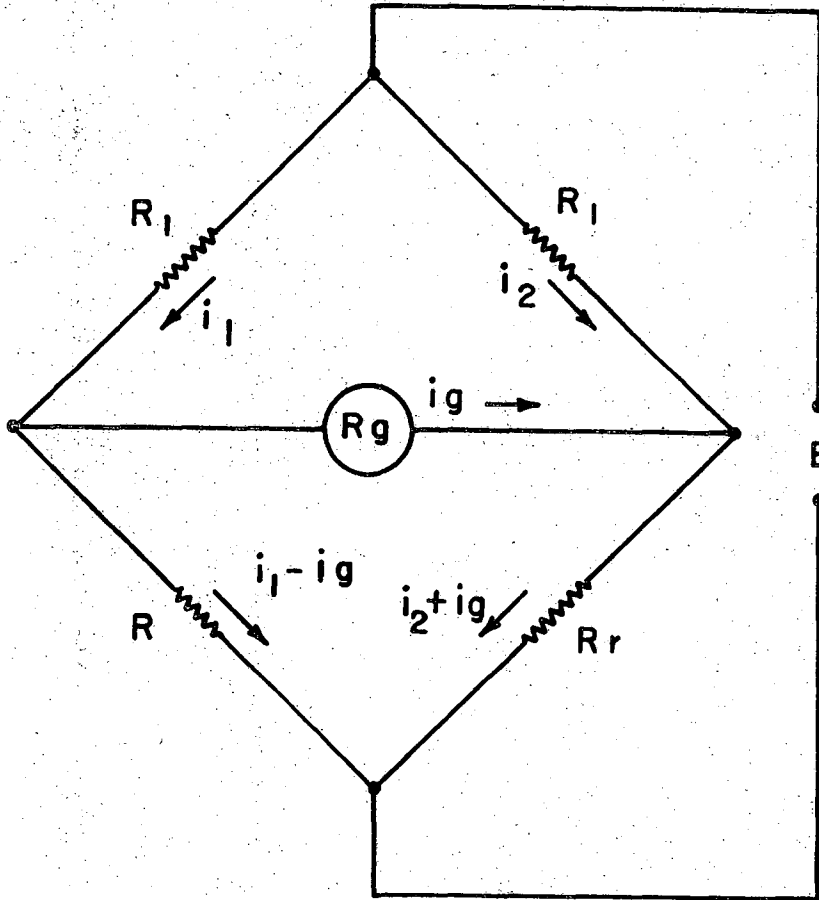
Then,

$$E = i_1 R_1 + (i_1 - i_g) R \tag{1}$$

$$E = i_1 R_1 + i_g R_g + (i_2 + i_g) R_r \tag{2}$$

$$E = i_2 R_1 + (i_2 + i_g) R_r \tag{3}$$

Solving (1) for i_1 and substituting in (2), then solving (3) for i_2 and substituting in (2), then solving the resulting equation for i_g , and finally substituting



XBL718-4039

Fig. 9. Bridge circuit.

$$R = R_r + \Delta R$$

we have the current in the galvanometer to first order, in ΔR .

$$i_g = \frac{EAR}{2R_1R_r + 2R^2 + R_1R_g + 3R_rR_g}$$

The voltage across the galvanometer is

$$E_g = i_g R_g$$

Substituting in numerical values from Fig. 5,

$$R_1 = 23.5k\Omega$$

$$R_r = 1k\Omega$$

$$R_g = 0.8k\Omega$$

we have that

$$E_g = EAR \times \frac{0.8 \times 10^{-3}}{2(23.5)(1) + 2(1)(1) + (23.5)(0.8) + 3(1)(0.8)}$$

$$E_g = 1.33 \times 10^{-5} EAR$$

We know that $\Delta R = \alpha R \Delta \theta$ where α is the temperature coefficient of resistivity of the thermistor, in this case, $0.04/^\circ C$. So

$$E_g = 0.00053E\alpha\Delta\theta$$

The calorimeter normally operates at 1/3 voltage, so $E = 1.35/3 = 0.45$ V.

Thus,

$$E_g = 0.00024 \Delta\theta = 2.4 \times 10^{-4} \Delta\theta$$

The sensitivity of the Leeds and Northrup HS type 2290 galvanometer is 10^{-11} amp/mm at 1 meter, and its coil resistance is 800Ω , so its sensitivity is 8×10^{-9} V/mm. The expected temperature rise has already been calculated in Sec. C2 as 0.04°C , so

$$E_g = 9.6 \times 10^{-6} \text{ V}$$

The deflection of the galvanometer beam with this rise in temperature of the sample-holding thermistor is therefore

$$\delta = \frac{9.6 \times 10^{-6} \text{ V}}{8 \times 10^{-9} \text{ V/mm}} = 1.2 \times 10^3 \text{ mm} = 1.2 \text{ m}$$

The actual path length was three meters so that the effective deflection at the position of measurement was three times the value of δ above.

$$\delta_{\text{effective}} = 3.6 \text{ meters}$$

Of course there was no actual galvanometer deflection, since the photocell circuitry supplied an equal but opposite current to maintain the null position.

It is obvious from these calculations that the galvanometer in question is sufficiently sensitive for the measurement.

The physical arrangement of the photocells and galvanometer is similar to that shown in the circuit diagram and is shown in Fig. 10.

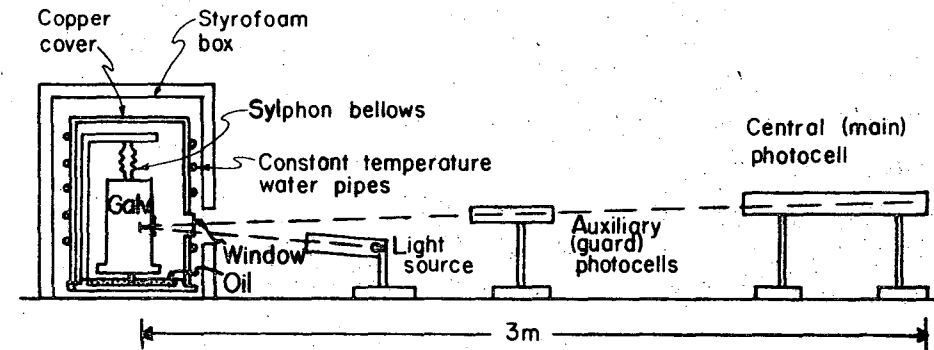


Fig. 10. Arrangement of photocells and galvanometer.

The central photocell is housed in a brass cylinder 18 inches long to prevent any light from affecting the galvanometer when the dark-room door is open. The room was kept dark while operating the calorimeter. Likewise, the two auxiliary photocells are at the rear of two tunnels about two inches apart drilled into an aluminum block about 5 inches long, with a groove between them which is lined up with the central photocell.

The galvanometer is supported in a stand on a sylvon bellows to prevent the tipping of the building (a few seconds of arc) from altering the zero point. A plate mounted below the galvanometer is immersed in oil to provide some damping for the suspended galvanometer housing. Covering the galvanometer and stand is a copper housing with about five turns of copper tubing soldered to the outside, through which circulates water from a constant temperature bath. A styrofoam box fits over the copper housing.

d. VTVM and recorder. Block 4 contains the portion of the circuit which measures and records the signal from the battery which keeps the galvanometer centered. The switch and the series of three $2M\Omega$ resistors is a means for applying different time constants to the signal and smoothing out small very short term fluctuations. The D.C. vacuum tube voltmeter is a Hewlett-Packard model 412 A. The recorder is a Leeds and Northrup recording millivoltmeter, Speedomax model G.

e. Vacuum system. The calorimeter must operate at a high vacuum to prevent massive heat losses from the sample-holding thermistor by air conduction. A vacuum line with a mechanical fore pump, three mercury

diffusion pumps, and a liquid nitrogen trap was used. This system was capable of evacuating the calorimeter vessel to 10^{-6} Torr in three to four minutes.

f. Constant temperature bath. For maximum stability, a constant temperature medium must surround the temperature-sensitive components of the calorimeter. A temperature controller based on the Wheatstone bridge was designed and constructed and used to regulate the temperature of a 34 liter water bath. The bath vessel was a glass battery jar contained in a large cardboard box with about two inches of thermal insulation between box and jar to insulate the bath from fluctuations in room temperature. The bath was kept in continuous vigorous motion by a mixer. Cooling was provided by about 10 feet of plastic tubing coiled on the bottom of the jar, through which tap water circulated at a rate which could be varied according to the amount of cooling needed. Heating was provided by a 250 watt heat lamp directed through the side of the battery jar onto an aluminum deflector plate inside the water bath. The aluminum plate thus served as both a heat source for the bath and a thermal shield to prevent the calorimeter vessel from being heated directly by the heat lamp. The temperature control circuit used varied the output power of the heat lamp continuously as required to maintain the operating temperature rather than simply turning the heat lamp on and off at full power. The temperature sensing element used was a resistance thermometer--Hallikainen model 1106A. With this control system the operating temperature of the water bath could be held to $25.005 \pm 0.001^\circ\text{C}$, as measured with a calibrated Beckman thermometer.

C. Operating Procedure

The evolution of the operating procedure for the calorimeter was not especially straightforward. Initially, when a matched set of thermistors in a mount was plugged into the connector in the calorimeter vessel, the outer copper cover was screwed on directly over the thermistors. The vessel was lowered into the constant temperature bath and the system was evacuated to approximately 10^{-6} Torr. The bridge was then turned on to 1/3 battery voltage and the recorder was started. Typically, about 80 minutes were required for a straight base line to be reached. This delay was intolerable, in view of the 26.5 minute half life of the isomer. In order to determine the factors responsible for this result, the vacuum was left undisturbed, but the calorimeter vessel was raised out of the constant temperature bath for several minutes. When the bridge was turned on again, 80 minutes were required to reach a straight base line. Next, the vessel was left in the bath and let down to air for several minutes. When a vacuum was re-established and the bridge was turned on, only twenty minutes were required for a flat base line to be reached. Simply turning the bridge off, then on again, under normal running conditions produced almost no effect on the base line. Thus it was shown that the instability of the calorimeter was not due to slowness of the vacuum system in evacuating to 10^{-6} Torr, but was a temperature effect of some sort.

In addition, a wild deflection of the galvanometer beam occurred when an ice cube was held against the outer copper cover, even though the apparatus was in the constant temperature bath and the pressure within the calorimeter was down to 10^{-6} Torr. This was a most surprising result.

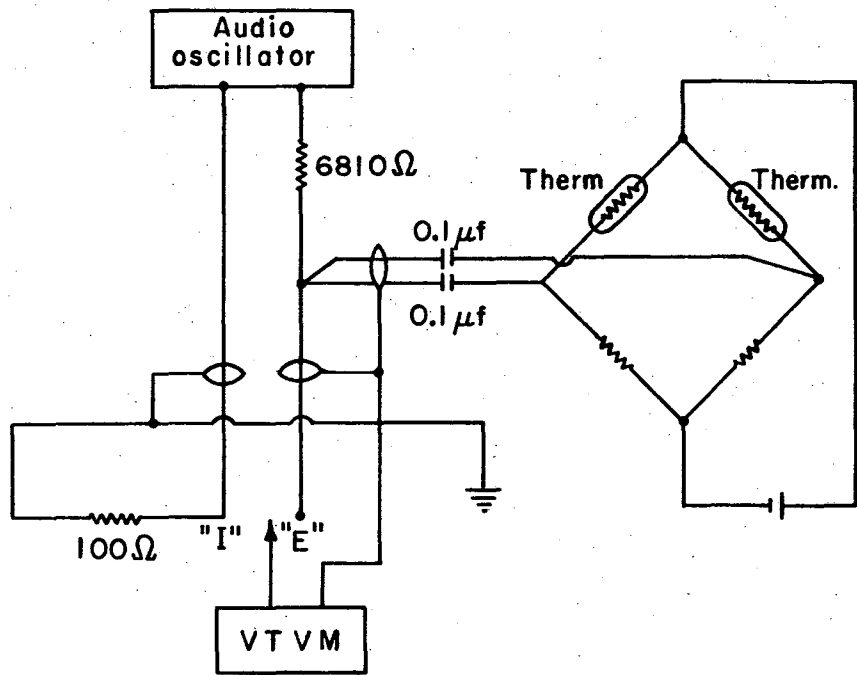
It demonstrated the need for a heat radiation shield around the thermistors, since conduction of heat along the leads could not account for such an effect. Accordingly, a small aluminum cap, shown in Fig. 7, was constructed to fit directly over the thermistors. As expected, the addition of this cap eliminated the large deflection produced by the ice cube treatment.

1. Use of Helium

The problem of the large thermal inertia of the system which produced the initial delay in reaching a flat base line was eliminated by admitting a small amount of helium into the calorimeter for several minutes after the fore pump vacuum had been established. Only then was the diffusion pump used to evacuate the calorimeter to 10^{-6} Torr. This procedure speeded the attainment of thermal equilibrium between calorimeter and water bath, and the flat base line could be obtained in only 20 minutes. Helium was shown to be far superior to air for this purpose.

2. Heating Phase

It seemed that much of this residual delay of twenty minutes might be due to a slow outgassing of the thermistors in the high vacuum, so a circuit was devised whereby a 20KHZ signal from an audio oscillator might be fed into both thermistors in order to heat them to about 70°C while they are in the calorimeter vessel under high vacuum. This heating circuit is shown in Fig. 11. The A.C. signal is applied at the points marked "audio osc. (A)" in the circuit diagram, Fig. 5. A vacuum tube voltmeter (Hewlett Packard, model 400 D) monitors the signal at points



XBL718-4040

Fig. 11. Heating circuit for thermistors in the calorimeter.

"I" and "E" to obtain the current and voltage, respectively, flowing through the thermistors. From this information their approximate resistances may be calculated. Since the resistances of the thermistors at 70°C have previously been measured, the amplitude of the audio oscillator may be adjusted upward until these resistances are obtained, thus preventing the overheating of the thermistors.

When the thermistors were heated in this way during the last few minutes of the helium treatment and for several minutes after the helium had been evacuated, a flat base line could be obtained in about 14 minutes.

One further refinement was made when it became apparent that the galvanometer beam could not be contained by the two auxiliary photocells whenever the thermistor mount was removed. The 1K resistors with a wire between them leading to ground were soldered to the terminals of an Amphenol 83-22SP connector, and this was inserted at points "A" before removing the thermistors from the circuit.

D. Calibration of Calorimeter

The calorimeter was calibrated by passing a 20KHZ signal from the audio oscillator into the left thermistor (the sample-holding thermistor) at the point marked "audio osc. (B)" in the circuit diagram and measuring the deflection produced on the chart. The voltage of the signal applied to the thermistor was measured by the A.C. voltmeter. The resistance of the thermistor was measured to the nearest ohm by comparison to a decade resistance box in a Wheatstone bridge circuit. Knowing the resistance of the thermistor and the A.C. voltage across it, the power dissipated in it

may be calculated. Thus, chart deflection as a function of power dissipated in the sample-holding thermistor is readily obtained.

Several tests were made to insure the suitability of this calibration procedure. First, the A.C. voltage across the reference (right hand) thermistor was measured while the A.C. calibration signal was being applied to the left thermistor. There should be no leakage, and, indeed, no voltage could be detected with a system capable of detecting 1 μ v.

Second, the frequency of the calibration signal was varied while the amplitude was held constant. The chart deflection did not change with changing frequency, thus showing that all A.C. shunts were working properly, and the system was insensitive to frequency changes.

Third, the D.C. voltage of the bridge was measured with and without the presence of the A.C. calibration signal. It remained constant, eliminating the possibility that the calibration signal was being partially rectified in passing through the thermistor or any other part of the circuit.

III. CHEMISTRY

A. Solvent Extraction

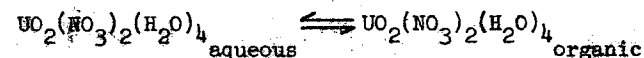
1. Theoretical Considerations

a. Introduction. The solubility of uranyl nitrate in organic solvents has long been recognized, and the ability of diethyl ether to extract this salt has been used in systems of analysis for many years. In 1842 Peligot¹⁰ found that uranyl nitrate dissolved readily in diethyl ether, and he used this solvent in the purification of uranium from pitchblende. More recently, separation of uranium from other elements by organic extractants has assumed great importance in connection with the development of atomic energy.¹¹ Extraction of uranium from water solutions is small, however, unless the concentration of uranium is large or unless the composition of the aqueous phase is altered in such a way as to render the uranium more soluble in the organic solvent.¹²

Because uranium has vacant d and f orbitals in its electronic structure, it will accept a certain number of electron pairs and form co-ordination complexes with Lewis bases, notably water and other oxygen-containing solvent molecules. The usual number of co-ordination positions around the uranyl cation is six, and it is hexahydrated in pure water.¹³

In the extraction of uranyl nitrate from an aqueous medium by an organic solvent, the complex most easily soluble in the organic phase is the di-nitro tetra-hydrate, $UO_2(NO_3)_2(H_2O)_4$, rather than the hexahydrate, since water molecules, being highly polar, are not compatible with a non-polar organic phase.

A distribution constant, K_D , may be defined for this complex:



$$K_D \equiv \frac{[\text{UO}_2(\text{NO}_3)_2(\text{H}_2\text{O})_4]_{\text{organic}}}{[\text{UO}_2(\text{NO}_3)_2(\text{H}_2\text{O})_4]_{\text{aqueous}}}$$

A better measure of the overall success of the extraction is the distribution ratio, D , defined as the ratio of the uranium concentration in the organic phase to that in the aqueous phase:

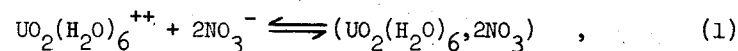
$$D \equiv \frac{[\text{U}]_{\text{organic}}}{[\text{U}]_{\text{aqueous}}}$$

This is a stoichiometric ratio, including all species of the uranium in the respective phases, and as such is difficult to predict, since the K_D of each species must be known.

A simpler and quite adequate analysis of the extraction may be made by assuming that the $\text{UO}_2(\text{NO}_3)_2(\text{H}_2\text{O})_4$ complex is the only extracted species. Since K_D must by definition remain constant, an increase in the concentration of the complex in the aqueous phase will result in a greater extraction into the organic phase; and similarly if the complex is altered in the organic phase, by replacing co-ordinated water with solvent molecules, for instance, more of the original species must be extracted from the aqueous phase to maintain the K_D .

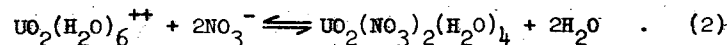
b. Aqueous phase. Reactions in the aqueous phase which lead to greater concentration of $\text{UO}_2(\text{NO}_3)_2(\text{H}_2\text{O})_4$ will be considered first.

In a solution of low to moderate ionic strength the uranyl hexahydrate is the predominant species:



where $(\text{UO}_2(\text{H}_2\text{O})_6, 2\text{NO}_3)$ represents a uranyl cation with water molecules occupying the six co-ordination positions of the uranium atom and two nitrate ions held to the complex loosely by simple electrostatic attraction.

If, however, the activity of the water is low and the nitrate concentration is high the reaction is:



Two nitrate ions have replaced two water molecules in the co-ordination sphere. The law of mass action predicts that addition of nitrate ion to the aqueous phase will shift the equilibrium represented by Eq. (2) to the right, with the formation of more of the extractable nitrate complex. In addition, the distribution ratios for uranium vary with the nature of the nitrate used, as well as with total nitrate concentration.¹⁴ The ability of various nitrates to "salt out" uranium--that is, to force uranium into the organic phase--has been related to the hydration of the cation,¹⁵ the activity coefficient of the pure nitrate salt,¹⁶ and the radius and charge of the cation.¹⁷ It would seem that the principal effect is the binding of water around the cation in a shell of oriented water dipoles, thus lowering the water activity, and shifting the equilibrium of Eq. (2) toward formation of the $\text{UO}_2(\text{NO}_3)_2(\text{H}_2\text{O})_4$ complex. Specifically, cations of small ionic radius and large charge, such as Zn^{++} , Mg^{++} , and Al^{+++} , are powerful salting-out agents as nitrates.

Anions other than nitrate that complex uranium in the aqueous phase may seriously interfere with the extraction, notably chloride, fluoride, sulfate, and phosphate.¹⁸ The adverse effects of these anions may be eliminated by removing them from solution prior to the extraction, or minimized by complexing the anions with cations of salting-out agents or by simply using an excess of an efficient salting-out agent to override the anion interference. Fluoride ion is complexed by aluminum and calcium; sulfate and chloride ions are complexed by ferric ion; phosphate ion is complexed by ferric and aluminum ions.

The addition of nitric acid to the aqueous phase promotes the extraction of uranium by preventing the hydrolysis of uranyl ion and by increasing the concentration of nitrate. An acid medium is also essential to the stability of the ²³⁹Pu stock solution.

c. Organic extractant. The selection of the most suitable organic extractant is no less important than the treatment of the aqueous phase. Since the organic phase must undergo subsequent treatment to obtain the uranium, however, additional factors such as speed and ease of handling must be considered, in addition to the central question of extraction efficiency. Thus, the highly effective organo-phosphorus compounds, notably tri-butyl phosphate (TBP) and tri-octyl phosphine oxide (TOPO), do not allow the very rapid recovery of virtually mass-free uranium which is essential to the success of the extraction. Attention must be confined to the more volatile organic solvents.

In principle, uranium may be back-extracted from the organic phase into a highly dilute acid phase. In practice, however, the yield was not good, and the resulting volume of solution was too large.

Returning to the equation

$$K_D = \frac{[\text{UO}_2(\text{NO}_3)_2(\text{H}_2\text{O})_4]_{\text{org}}}{[\text{UO}_2(\text{NO}_3)_2(\text{H}_2\text{O})_4]_{\text{aq}}}$$

it may be seen that any reaction of the extracted species in the organic phase, such as polymerization, dissociation, or chemical combination with the solvent itself, tends to reduce the activity of the extractable species in the organic phase, and the overall extraction equilibrium is shifted toward a higher distribution ratio, D. ($D = \frac{U_{\text{org}}}{U_{\text{aq}}}$).

Oxygen-containing organic liquids will serve as solvents for a number of metal salts because the basic (electron-donating) character of the oxygen atom promotes the incorporation of solvent molecules into the co-ordination sphere of the metal ion. This results in a complex which bears a closer structural resemblance to the organic liquid and which is therefore more soluble in that liquid than is the aqueous metal salt complex. Alcohols, ethers, and ketones in which the oxygen atom has a high electron density and is unhindered by bulky hydrocarbon groups should be effective solvents for uranyl nitrate. In order to estimate the metal co-ordinating ability of various oxonium solvents (and thus their effectiveness as solvents), Katzin, Simon, and Ferraro¹⁹ have made a study of the heats of solution of uranyl nitrate in some of these oxonium solvents. Their results indicate that diethyl ether is the strongest base of the ethers tested and compares well with the alcohols. It may be evaporated very rapidly to a small volume, an important factor.

2. Experimental Extraction Work

a. Choice of salting-out agent. Since aluminum nitrate had previously been used in this laboratory as a salting-out agent for the ether extraction of uranium, it was assumed that it would be a suitable salting-out agent for the present work. However, it became apparent when the extraction yields were closely examined that such was not the case. The yields were erratic and seldom as high as the 90% which was expected. They averaged $72 \pm 25\%$, which is much too low for such a straightforward process.

This and the following extraction yield studies were made by shaking 125 ml of the appropriate aqueous salt solutions, which were also 1M in nitric acid and contained tracer uranium-233 and ferrous sulfamate, with an equal volume of diethyl ether which had been pre-equilibrated with the same salt. (See discussion in Sec. 2c.) All extractions were done at room temperature. After the extraction the ether was scrubbed once with a fresh solution of the salt in 1M nitric acid, evaporated to dryness, taken up in concentrated nitric acid and run through the nitric-hydrochloric acid anion exchange column described in Sec. B2, ion exchange. Uranium yields were determined by alpha counting. The yield of this column is $88 \pm 2.2\%$, and the extraction yields have been corrected for this factor.

Hyde²⁰ and Kuznetsova, et al.²¹ recommend magnesium nitrate as a salting-out agent for uranium. Hyde reports 99% extraction from a solution 2.5M in magnesium nitrate and 0.5M in nitric acid and 38% extraction from a 1.55M magnesium nitrate-0.5M nitric acid solution, while Kuznetsova, et al. report a 90% yield from a 0.3M magnesium nitrate solution. With this wide discrepancy in results, perhaps it is not surprising that

neither was duplicated in this work. Yields for the extraction from magnesium nitrate-nitric acid were $76.1 \pm 6.6\%$.

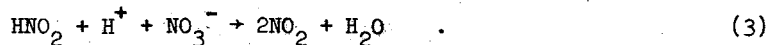
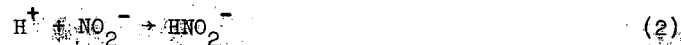
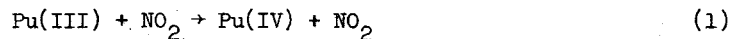
Furman, et al.²² noted that the distribution coefficient from a saturated solution of zinc nitrate was the highest that was observed in an extensive study of salting-out agents for the ether extraction of uranium--99.6%. This excellent yield was confirmed in the present work, extraction yields averaging $93.6 \pm 10.2\%$.

b. Reducing agent for plutonium. A diethyl ether extraction from an aqueous plutonium phase saturated with zinc nitrate was therefore chosen to obtain the uranium-235m. Since both plutonium(IV) and plutonium(VI) are also extracted under these conditions, the basis for the separation is the fact that Pu(III) is practically inextractable at any nitrate concentration. This is undoubtedly due to its much lower tendency to form nitrate complexes. There is a wide choice of reducing agents to effect the reduction of Pu(IV) to Pu(III). (Hindman²³ has found the Pu(III)--Pu(IV) potential in 1M nitric acid at $25 \pm 3^\circ\text{C}$ to be -0.916 ± 0.006 volt.) In the Redox process, which is a solvent extraction process for the recovery and separation of U and Pu from irradiated reactor fuels, ferrous sulfamate, $\text{Fe}(\text{SO}_3\text{NH}_2)_2$, is used to reduce Pu(IV). It has advantages over other reductants, namely, stability, ease of preparation, fast rate of reduction and minimum interferences with subsequent recovery operations. It was chosen as the reducing agent for this extraction, and it was prepared by dissolving iron powder in an aqueous solution of sulfamic acid and drying the product under a nitrogen atmosphere to prevent oxidation to ferric sulfamate.

c. Plutonium chemistry. In practice it was found that the optimum conditions for the extraction of uranium were not compatible with preservation of a stable solution of Pu-239 in the III state. Specifically, after several ether extractions were made from a Pu(III) stock solution 1M in nitric acid and saturated with zinc nitrate, the stock solution changed in color from the royal blue of the Pu(III) to a muddy green, and a tan precipitate formed on the walls of the container. There was also some evolution of gas from the solution.

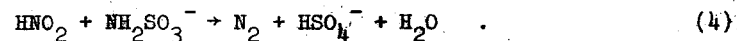
A solution of Pu(III) in 1M HNO₃ is quite stable, however, which indicates that the problem lies with the addition of aluminum nitrate or the ether extraction. It was felt that both factors contributed to the deterioration of the Pu(III) stock solution.

The Zn⁺⁺ ion is very strongly hydrated in aqueous media because of its large positive charge, and because it binds so many water molecules to itself, it will greatly lower the activity of the water in such a system. In the Pu(III) stock solution, the effect of the lower water activity is to raise the effective concentration of nitric acid. A high nitric acid concentration is a source of oxidant (probably nitrite) which tends to reoxidize Pu(III) to Pu(IV). The observation that the stock solution remained stable for several days and then deteriorated rapidly is consistent with the autocatalytic mechanism proposed by Brunstad for the oxidation of Pu(III) by nitrite impurities in nitrate solutions.²⁴



Latimer²⁵ states that "concentrated nitric acid is a rapid and powerful oxidizing agent," whose oxidation potential rises rapidly with increasing acid concentration.

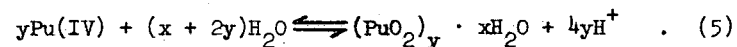
The initial stability of the stock solution was attributed to the presence of the sulfamate ion, NH₂SO₃⁻, which may be oxidized by nitrous acid, thus removing the oxidant and preserving the Pu(III).



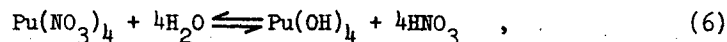
When the sulfamate is exhausted, the oxidation proceeds as in Eqs. (1), (2), and (3). This mechanism was supported by the observation of bubbling (N₂?) in the stock solution of Pu after it was saturated with aluminum nitrate.

Assuming that the Pu(III) is oxidized to Pu(IV), the ether extractions performed on the stock solution become important. It is well known that ether will extract significant amounts of nitric acid from aqueous media, and it is likely that the pH of the stock solution was raised to the extent that the Pu(IV) hydrolyzed. Successive hydrolysis reactions of Pu(IV) result in a colloidal polymeric form of quadrivalent Pu, which is easily recognized by its emerald green color. Whenever the acid concentration is less than 0.1M the presence of polymeric Pu(IV) should be suspected. High Pu concentration and elevated temperature result in polymerization at even higher acidities.

Polymerization is thought to occur as follows.²⁶

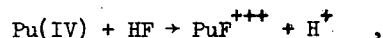


Other authors^{27,28} give the reaction as



but Brunstad later cites X-ray diffraction data which indicate that quadrivalent plutonium "hydroxide" is really hydrated plutonium dioxide.²⁹

The polymer is extremely stable, and Eq. (5) proceeds until the acidity of the supernatant solution is high enough to stabilize the monomeric Pu(IV) in solution. The association constant for the Pu(IV) polymer is not known, but both Miner³⁰ and Costanzo and Biggers³¹ report that neither fluoride nor sulfate ions, both of which complex Pu(IV) strongly, will prevent polymerization. Complex formation and hydrolysis are competing reactions and may be looked upon as the displacement of the water molecules from the hydration sphere by the anionic ligand or by OH^- , respectively. The association constant for the Pu(IV) polymer must, therefore, be greater than that for the fluoride complex,



which is given by McLane as 1.7×10^4 in 1M nitric acid.³²

A further indication of the stability of the polymer is given by the observation that polymer is formed and persists when solutions of Pu(IV) are diluted with water, because of transient regions of high pH, even though the final acidity may be high enough to prevent polymer formation.

It is not known whether uranium formed from polymeric Pu-239 will escape from the polymer matrix, and almost certainly that formed from

solid PuO_2 will not enter solution. Ether extractions done on Pu stock solutions containing appreciable amounts of either substance will surely give a low yield of uranium. Thus it was necessary to destroy the polymer and the PuO_2 which were present. Depolymerization is very slow at room temperature in moderate acid concentrations. The rate may be increased by heating, stronger acid concentration and the addition of strong complexing agents such as fluoride or sulfate. Both Miner³³ and Costanzo and Biggers³⁴ report a 50% conversion time of several minutes at 25°C with an acid solution containing 0.05M F^- and 0.2M $\text{Al}(\text{NO}_3)_3$. PuO_2 which has not been strongly ignited may be dissolved in hot concentrated nitric or sulfuric acid. Since sulfate is added to the Pu stock solution in the peroxide precipitation step of purification and concentration, it was decided to use sulfate as the complexing agent in destroying the polymer. Both sulfate and fluoride interfere with the extraction of uranium, but any sulfate which remains after peroxide precipitation will be complexed by ferric ions, which are present after Pu(IV) has been reduced to Pu(III) by ferrous sulfamate.

The procedure for conversion of the polymer to Pu(IV) was the following. Polymeric and precipitated Pu were evaporated to dryness by a "Cal Rod" heating unit placed in the solution. The temperature of the liquid was maintained between 80 and 90°C by a Variac placed between the heater and the line voltage. Nitric acid at 10 - 12 M was added to the resulting solid, along with several ml of 12M H_2SO_4 per 500 ml of HNO_3 , and the mixture was heated at 70 - 80°C for a few days. The bright green appearance of the solution caused some consternation until it was found that dilution to 4 - 5M in HNO_3 resulted immediately in the usual brown

color of Pu(IV). A small amount of brown Pu(IV) placed in concentrated HNO_3 turned bright green, the brown color returning upon dilution. The color change from green to brown occurred far too rapidly to involve the polymer, and in addition the polymer should not form in concentrated acid. The green solution obtained in concentrated HNO_3 was therefore attributed to the formation of a green Pu(IV)-nitrate complex at high nitrate concentration.

d. Plutonium peroxide precipitations. In order to reduce the volume of the ^{239}Pu stock solution obtained in this procedure and to eliminate contaminants, peroxide precipitations were then done. This procedure must be undertaken with great care, as the plutonium peroxide precipitated from the nitrate stock solution used in this experiment is unstable at room temperature. The decomposition is autocatalytic, occurring rapidly and with considerable foaming if conditions are not carefully controlled, hence the careful chilling of the reactants, the chilling of the peroxide after precipitation, and the necessity to centrifuge the mixture at the full speed of the centrifuge so that the supernatant may be removed before the plutonium peroxide warms up enough to decompose.

Not more than 10 cc of the plutonium stock solution are placed in a 40 cc centrifuge cone with about 1/2 cc concentrated H_2SO_4 and heated in a hot water bath at 65°C until any precipitate is dissolved. The plutonium solution is then chilled in ice water for thirty to forty-five minutes, as is 15 cc of H_2O_2 . The peroxide is poured into the plutonium solution, the resulting precipitate is stirred briefly, and the tube is set back into the ice bath for three minutes. Then the tube is covered with parafilm and centrifuged at top speed for two minutes.

It is removed from the centrifuge immediately and the supernatant liquid is decanted. The decomposition of the plutonium peroxide will begin as the precipitate warms up, and it must be quenched periodically by placing the tube back into the ice bath until the foaming subsides. When the olive green peroxide has decomposed into the dark blue III state or the brown IV state solution, the reaction is complete.

Obviously, a method must be found for maintaining a stable Pu(III) stock solution from which many ether extractions may be made without deterioration. Acid and salt extraction by the ether, with attendant polymer formation by Pu(IV), may be prevented by pre-equilibration of the ether with an aqueous solution which is as close as possible to the composition of the Pu stock, that is, 1 - 2M in HNO_3 and saturated with zinc nitrate. The ether will be saturated with acid and $\text{Zn}(\text{NO}_3)_2$ before it reaches the Pu solution and will be unable to extract any additional acid or salt.

The problem of preventing the oxidation of Pu(III) to Pu(IV) was not so easily solved. The sulfamate ion was not sufficient as a holding reductant, and it was impossible to re-reduce the Pu stock to Pu(III) with any of a number of reducing agents (ferrous ion, ascorbic acid, hydroxyl amine, hydrazine, hydroquinone, HI), once deterioration had begun. Peterson and Wymer³⁵ suggest hydroxylamine and ferrous sulfamate as holding reductants, but addition of hydroxylamine to the Pu(III) stock had little effect on its keeping properties. After a process which might best be described as trial and error, the following sequence was devised. To a Pu(IV) solution 1M in HNO_3 ferrous sulfamate is added in small increments with agitation for a minute between additions until the Pu(IV)

is reduced to Pu(III). The solution is made 0.3M in sulfamic acid and 0.05M in hydroxylamine by adding the solid reagents. Finally the solution is saturated with zinc nitrate. After about ten days several grams each of ferrous sulfamate and hydroxylamine are added. In ten more days, or whenever the Pu(III) stock solution begins to depart from its royal blue color, several grams each of ferrous sulfamate, hydroxylamine, and sulfamic acid may be added. The useful life of a Pu(III)-zinc nitrate solution treated in this manner is limited mainly by the volume increase after each ether extraction. After four extractions it was necessary to subject the plutonium stock solution to a series of peroxide precipitations.

e. Ether-associated peroxides. Very early in the preliminary extraction work it was repeatedly and violently demonstrated that unstable substances were present in the ether after contact with the nitric acid--salt solutions. As the ether was evaporated to a small volume in the hot water bath it became red-brown in color and exploded, with evolution of nitrogen dioxide. The darkening in color was rapid and usually occurred when the volume reached one or two ml. This state of affairs was obviously intolerable, both from the standpoint of greatly reduced yields and of the danger involved when the ether contained plutonium and uranium. The ether used in the experiment was "Baker Analyzed" reagent grade anhydrous ether. Samples of this ether that had been stored in darkness and in room lighting were evaporated to dryness without any explosion, raising the likelihood that explosive peroxides were formed during contact with the aqueous stock solution. Feinstein³⁶ reported a process for removing

peroxides from ether, which consisted of contacting the ether with a strong base anion exchanger in the free base form. Peroxides were absorbed by the resin.

Three grams of Dowex AG-1 X-8 resin were converted to the free base form by washing with several liters of 4M NaOH until a negative test for chloride was obtained from the washings. Then ether which had been shaken with 1M HNO₃ - salt solution was mixed with the resin to effect removal of peroxides. Upon evaporation to a small volume, this ether also exploded.

Red fuming HNO₃ was added to the ether at a point before the explosion occurred in an attempt to destroy the unstable component, but this, too, resulted in an explosion.

Hydriodic acid was added to the ether during the evaporation. Free iodine was formed and the explosive reaction, though it still occurred, was much subdued. It was found that addition of 1 ml of 55% HI to the ether after it had been evaporated to 10 ml was sufficient to reduce the explosion to a vigorous bubbling and evolution of nitrogen dioxide.

B. Ion Exchange

A sample of uranium prepared by an ether extraction of the Pu(III) stock solution and evaporation of the ether to dryness with HI was placed on one of the thermistors in the calorimeter. A very large imbalance of the bridge was observed, and several hours were required for equilibrium to be established. The sample placed on the bead was not mass-free, and the bead was liberally coated with the material, which

must have increased the thermal inertia of system greatly. Since the performance of this set of thermistors was normal in subsequent tests after removal of the sample, it was assumed that the long time required for equilibrium to be established was a direct result of the sample material on the bead and not due to a defect induced in the thermistor itself. The main constituent of the mass was undoubtedly iron, due to the use of ferrous sulfamate as a reductant for the Pu(IV) and the extraction of ferric ions by the ether. It seemed appropriate, therefore, to devise a procedure for removing iron from the uranium. A method which has been widely used for micro-chemical separations of this sort is anion or cation exchange.

1. Theoretical Considerations

a. History. Ion exchange as a chemical tool has a long and interesting history, with scattered references extending from the Old Testament to the discovery of ion exchange in soils in 1850. The spectacular modern day evolution of ion exchange methods began in 1935 when Adams and Holmes found that crushed phonograph records exhibit ion exchange properties.³⁷

Nearly all the ion exchange media in current laboratory and industrial use are organic resins whose subsequent development was due to these early experiments with this most unlikely material.

b. Description of resin structure. Ion exchangers are insoluble solid materials which carry mobile cations or anions that may be exchanged for a stoichiometrically equivalent amount of other ions of the same sign when the exchanger is in contact with an electrolyte solution. They owe this characteristic feature to their rather unique structure, which

consists of a framework held together by chemical bonds, and carrying a positive or negative charge. The surplus charge is compensated by ions of the opposite charge which are free to move throughout the framework and exchange with other ions of the same sign. The framework of a cation exchanger may be regarded as a macromolecular polyanion, that of an anion exchanger as a polycation. Organic ion exchange resins consist of a polymerized cross-linked hydrocarbon matrix, such as styrene-divinylbenzene or a polyacrylate, to which have been affixed ionic groups. Examples of such groups are sulfonate or carboxylate ions for cation exchange and substituted ammonium ions for anion exchange.

If a metal ion is to be absorbed on an ion exchange resin, it must, of course, have the same sign as the mobile ion it will replace. A cation such as the uranyl ion, UO_2^{++} , may be absorbed on an anion exchange resin only if it forms an anionic complex in the solution used on the column. Thus the uranyl ion will be absorbed by such a resin from both hydrochloric acid and nitric acid solutions at high acid molarity, where it forms the complex $[UO_2(NO_3)_3]^-$.³⁸ In HCl, of course, the Cl^- complex is formed. Other workers propose that $[UO_2(NO_3)_4]^{--}$ is the absorbed species.³⁹ The ferric ion will be absorbed from hydrochloric acid, where it forms an anionic complex, but not from nitric acid.

c. Mechanism of exchange. The question of just why certain ions should replace the mobile anions or cations of exchangers still remains, however. It has been proposed⁴⁰ that the selectivity of ion exchangers is related to the degree of hydration of the exchangeable ions, rather than to a surface phenomenon or a chemical reaction. A small, highly charged ion will be strongly hydrated in a dilute aqueous medium. It will, therefore,

prefer the aqueous phase, since its transfer into the organic resin phase involves stripping away its sphere of oriented water molecules, which is an endothermic process. A large complex ion such as $\text{UO}_2(\text{NO}_3)_3^-$ is less hydrated, and therefore less energy is needed to remove its associated waters when it passes into the resin phase. Thus, in an exchange process, the larger, less hydrated ion is pushed into the resin phase so that the smaller ion can achieve maximum hydration in the dilute external phase.

A related factor is the difference between water-water interactions in the resin phase and in the aqueous phase. The dilute external aqueous phase has essentially the same hydrogen-bonded structure as pure water, and as such it tends to oppose the entrance of a large ion which breaks up a large volume of water structure but does not have sufficient charge density to bind and reorganize the water molecules. A small ion is able to orient water molecules around itself, essentially preserving the water structure. In the resin phase, however, the water structure is so badly disrupted that it offers less resistance to the intrusion of a large ion. In the exchange process, the large ion is ejected from the external aqueous phase into the less structured resin phase, with the limitation that the size of the ion must not be greater than the openings in the resin matrix.

Having proposed an explanation for the uptake of metallic ions by an exchange resin, one might now wonder how these ions are removed from the resin. This is usually accomplished by destroying the complex ion to which the metal owes its absorption. Uranium, for example, is removed from an anion exchanger by dilute hydrochloric or nitric acid due to

the dissociation of the anionic complex when the anion concentration drops. Conversely, uranium is removed from a cation exchanger by concentrated acid, since the anionic complex is formed under these conditions, and it will not be retained by a cation exchange resin.

2. Experimental Work

a. Description of materials and procedure. The columns used in these experiments were all of the following type. They were constructed of Pyrex glass tubing. The overall length was 13 centimeters, this length being divided into two portions--the lower portion, 5.5 cm, was constricted to a narrow tube approximately 2.5 cm in diameter which contained the resin; the upper portion, 7.5 cm in length, was wider, approximately 1 cm in diameter, and served as a reservoir for the solutions passing through the resin bed. To the bottom of the column was fused a small platinum tube, 6 mm long, with an inner diameter of about 0.2 mm. The drop volume was quite constant for the different columns, ranging from 0.013 cc/drop to 0.015 cc/drop.

All resins were supplied by Bio Rad Laboratories of Berkeley and were used without further purification except for conversion to various anionic forms as indicated.

The columns were loaded by inserting a glass wool plug into the column and washing a slurry of resin in the appropriate acid through the column until the resin level reached a mark about 0.5 cm below the constriction of the tube. A glass wool plug was placed on top of the resin.

The drop rate was controlled by pressure from a compressed air source applied to the top of the column through a tube inserted through

a cork stopper. A screw clamp on a second tube through the stopper was used to vary the air pressure.

All work was carried out at room temperature, due to the irreversible hydrolysis of the ferric ion at elevated temperatures.

In order to assess the separation properties of the various column materials, the samples placed on the columns were as similar as possible to the samples which would be obtained from ether extraction of the plutonium stock. They were prepared in the following manner. To 100 cc of a solution 1 N in HNO_3 and saturated with $\text{Zn}(\text{NO}_3)_2$ or some other inorganic nitrate was added several grams of solid ferrous sulfamate. This mixture was spiked with 10 λ of a uranium-233 tracer solution and shaken with 100 cc of ether for one minute. The ether portion was withdrawn and rapidly evaporated down to 10 cc in a hot water bath, then "scrubbed" with a few cc of the 1 N HNO_3 -saturated salt solution to which had been added a few grams of ferrous sulfamate. After centrifuging, the ether portion was withdrawn and evaporated down to about 2 cc, at which point 6 to 8 drops of 55% HI was added in order to destroy most of the explosive peroxides which caused spattering of the solution. Evaporation was continued over a bunsen burner until the volume was 1/2 cc. The sample was then cooled and placed on the column. More exact determination of column yields were made by placing 10 λ of the U-233 tracer in the appropriate solution directly onto the column. In this way, column yields were rendered independent of the extraction yield.

Solutions coming off the column were collected on platinum discs, evaporated and flamed. Inorganic mass was determined by inspection. Uranium yields were determined by alpha counting.

b. Cation exchange: Dowex 50W X-4 resin, 100-200 mesh was used. A chloride cation exchange column could be expected to separate iron from uranium in a concentrated hydrochloric acid solution, where uranium has little or no affinity for the resin, being found mainly as an anionic complex in these circumstances. ($[\text{U}_{\text{resin}}]/[\text{U}_{\text{aqueous}}] < 1$ for molarity > 6 .)⁴¹ At these higher acid concentrations iron would not be expected to remain on the resin either, since the ferric complex which exists at higher chloride concentrations is also negatively charged. Contrary to expectations, however, the distribution constant rises again after going through a minimum at an acid molarity of 4.⁴² In practice it was found that the iron is not quantitatively held on the resin at molarities of 10-12, and that although a relatively high yield of uranium was obtained, it was always contaminated with iron.

c. Zeolite. Zeolites were among the earliest materials used for ion exchange work, but the usefulness of these materials alone is quite limited, since they are stable in only a narrow range of pH. If, however, the zeolite is impregnated with tri-butyl phosphate, a basic extractant which has a notable affinity for the actinide elements, a useful column material results. When a mixture of ferric and uranyl ions in 6 molar nitric acid is passed through such a column the uranyl ions will be retained by the TBP-zeolite phase and the iron will not. The uranium may then be eluted by a mixture of 0.5 M nitric acid and hydrogen iodide, which reduces the uranyl to U^{4+} , allowing it to be removed from the TBP.

Although there was a clean separation from iron with this column and the uranium yield was 83% to 85%, the plates containing the uranium were consistently contaminated with inorganic mass from an unknown source, thus rendering the method useless as a cleanup of uranium.

d. Anion exchange: Except where stated otherwise, Dowex AG 1 X-8 resin, 100-200 mesh was used. Anion exchange resin may be converted to the acetate form by passing through it a concentrated acetate buffered solution. This resin may then be used to effect a separation of uranium from iron.⁴³ When the sample is loaded onto the column in a solution 0.01 M in acetic acid and 0.01 M in sodium acetate, the iron will pass through the column. Several column volumes of 8.7 M acetic acid are then passed through the column to remove the sodium acetate, which would, of course, be a source of mass, and the uranium is eluted with 0.8 M hydrochloric acid. The yields from this method tended to be rather low--typically 70%--and the plates containing uranium were contaminated with small amounts of iron.

It should be possible to separate uranium from iron using a chloride anion exchange column with a mixture of HCl and HF.⁴⁴ Iron will not be absorbed by the resin at HCl molarities below 1.0 (the HF concentration is 1.0 M), whereas uranium will be absorbed under these conditions. The uranium may then be eluted with 0.8 M HCl.

The results with this column were unpredictable and yields were generally low.

If the ferric ions can be reduced to ferrous, it is possible to separate uranium from iron on a chloride anion exchange column. Ferrous ions in an 8 M HCl solution do not form an anionic complex which can be absorbed by the resin, whereas uranyl ions do. The choice of reducing agents is quite limited, being confined to those which will not contribute to the mass of the uranium fraction. In addition, the reduction must occur within several minutes, as time is of the essence. Hydroxyl amine, oxalic acid, and hydrazine, for example, were far too slow. HI

and ascorbic acid reduced ferric to ferrous almost instantly, so columns were devised using these reductants.

When HI was used as a reducing agent, the sample was placed on the column in a solution 12 M in HCl and 7% in HI, washed with the same solution, and the uranium eluted with 0.1 M HCl.⁴⁵ The separation from iron was good but the yields were very low, ranging between 20% and 50%.

Ascorbic acid was then tried as a reducing agent for the ferric ions.⁴⁶ The best procedure for the separation was the following. The sample from the extraction was evaporated to dryness, and then dissolved in 0.25 cc of 4 N HCl, giving a pale yellow solution. Solid ascorbic acid was added until the solution became colorless (not more than 2 g/100 ml), and the sample was then placed on the column. The column was washed with a 4 N HCl-2% ascorbic acid solution, and the uranium eluted with 0.1 N HCl. With this method, column yields consistently above 80% were obtained, and the plates containing the uranium were quite free of any mass. However, when this column was used on a sample from an actual extraction from the plutonium-239, the results were erratic. This may have been due to the presence of impurities extracted from the stock solution of plutonium, since the initial addition of ascorbic acid resulted in dark-colored precipitates which could not be dissolved.

The search for a good clean-up column was resumed, the most promising prospect being a nitrate anion exchange column which had been tried previously with only moderate success. The uranyl ion forms an anionic complex in nitrate solutions. Iron, as ferrous or ferric, forms no nitrate complexes of this sort and thus is not absorbed at any nitrate concentration.

Previous columns gave good separation of uranium and iron but low yields, so attempts were made to improve the yield.

1) The anion exchange resin Dowex AG 1 X-8, 100-200 mesh which had been converted to the nitrate form with 8 N HNO₃ several months before gave poor results. Columns made of the same resin freshly equilibrated with 4 M HNO₃ gave yields of 67% - 72% consistently.

2) Higher yields were obtained with a slower drop rate (15-20 seconds per drop) than with a fast rate (10 seconds per drop). A balance must be struck here between the yield and the time required to run the column, which must be minimized.

3) Two resins of lower cross linkage, Dowex AG 1 X-2 and Dowex AG 1 X-4, were tried, and the yields were below 60%.

4) It was then reasoned that since the active sites of this anion exchange resin have a greater affinity for chloride than for nitrate ions, perhaps a dilute HCl solution would prove to be a better eluent than 0.8 M HNO₃. Results of this reasoning with the Dowex AG 1 X-8 mentioned above were erratic, but promising, the average yield being 80.5% ± 7.9%. An anion resin of higher cross linkage and smaller particle size, Dowex AG 1 X-10, minus 400 mesh was equilibrated with 4 N HNO₃ and used in the same column operation. Yields ranged from 87% to 92%, and the uranium-bearing plates, a total of 25 drops, were quite free of mass. The results were consistently good, and the uranium always appeared in the 19th to 33rd drops after the 0.1 M HCl was added to the column. The average yield was 88.8% ± 2.2%. This column had all the attributes needed for the separation, including a fairly short running time of 20-25 minutes. When an extraction of the plutonium-239 stock solution was prepared and used on the column, the results continued to be good and dependable.

IV. EXPERIMENTAL PROCEDURE

A. Extraction and Other Gloved Box Operations

Special gloved boxes were required for this experiment to reduce the danger of an explosion during the ether extraction of the plutonium. Two extra-large boxes were joined by a pass-through door, the primary extraction being carried out in one box, the clean-up of the sample in the other, less radioactive box. Provisions were made to flush the boxes with nitrogen during an extraction. With an initial nitrogen flow of 10 cfm for three minutes and a continuing flow of 1 cfm, the oxygen level could be reduced to three percent for the duration of the work in the boxes.

The interiors of the boxes were coated with epoxy paint to provide additional sealing at all joints and other metal interfaces. The half inch thick plastic front plate was attached to the box by angle brackets instead of screws to attempt to preserve the integrity of the box in the event an explosion did occur.

The stock solution for various runs consisted of from 10 to 20 grams of plutonium in a solution 2N in HNO₃ and saturated with zinc nitrate. Volumes ranged from 250 cc to 400 cc. The isotopic composition was:

²³⁹ Pu	95.89 atom %
²⁴⁰ Pu	3.93 atom %
²⁴¹ Pu	0.172 atom %
²⁴² Pu	0.00959 atom %

The plutonium was reduced to the Pu(III) oxidation state by ferrous sulfamate, with sulfamic acid and hydroxyl amine as holding reductants.

Approximately 200 cc of anhydrous ethyl ether were placed in a separatory funnel with an equal volume of an aqueous solution 2N in HNO_3 and saturated with zinc nitrate and shaken for at least two minutes to insure complete equilibration of the ether with the aqueous phase. The ether was drawn off and passed into the gloved box, as was 100 λ of uranium-232 in aqueous solution, which served as a tracer to determine the chemical yield of uranium. All the tracer and then half of the ether were added to the plutonium stock solution in a large separatory funnel. They were shaken vigorously for two minutes. The ether was withdrawn and placed in a beaker in a hot water bath. While this ether was evaporating, the second portion of ether was added to the stock solution and another extraction carried out in the same manner as the first. This ether was added to the first portion and was evaporated until the total volume reached approximately 30 cc, when it was removed from the hot water bath and placed in a large test tube for the "scrubbing" procedure.

In this operation a volume of 1N HNO_3 about half that of the ether was added to the ether, along with a few grams of solid ferrous sulfamate, and the test tube was shaken for 1 minute to reduce that Pu(IV) which had been extracted into the ether to the Pu(III) state. Then sufficient zinc nitrate to saturate the aqueous phase was added, and the test tube was shaken vigorously for two minutes to extract the Pu(III) back into the aqueous phase. Finally the mixture was centrifuged and the ether phase drawn off. Two such scrubs were performed on the sample in the first gloved box; the sample was then passed into the second box where three to five additional scrubs were done. Since the amount of plutonium extracted by the ether varied, the number of scrubs was determined by requiring that the aqueous portion of the last three

be free of the blue color of Pu(III). In this way no more than 10^6 dpm of plutonium were removed from the gloved box. After the final scrub the ether was evaporated in a hot water bath to 8 or 10 cc. At this point 1/2 to 1 cc of HI was added in order to destroy most of the explosive peroxides in the sample, and the evaporation was continued until the evolution of nitrogen dioxide ceased and the sample was about 1/2 cc in volume. The sample was passed out of the gloved box and placed in a hood, where all subsequent chemical operations were carried out.

B. Column

Evaporation was continued over a micro burner until the volume of the sample was 1/4 cc or less. An equal volume of 8 N HNO_3 was added to insure the proper normality, between 4 and 8 N, and the sample was placed on an anion exchange column to eliminate the Zn and Fe which were also extracted by the ether. The resin was Dowex AG 1 X-10, 400-mesh, which had been converted to the nitrate form by successive washings with 1N to 4N HNO_3 . The column arrangement has been described in Sec. III-B2. The drop rate was maintained at about 15 seconds per drop while the sample was loaded. The column was washed with about 5 cc of 4N HNO_3 at the faster drop rate of 10 seconds per drop. Drops 14 to 32 were taken on a small platinum plate, and evaporated under a heat lamp. The plate was lightly flamed to dispose of organic mass and also to serve as an additional uranium purification factor, since plutonium is not easily removed from a flamed plate.

C. Preparation of Sample

The uranium was removed from the plate with hot 2N HNO_3 , placed in a glass microcone and evaporated to 1 λ under a heat lamp. The

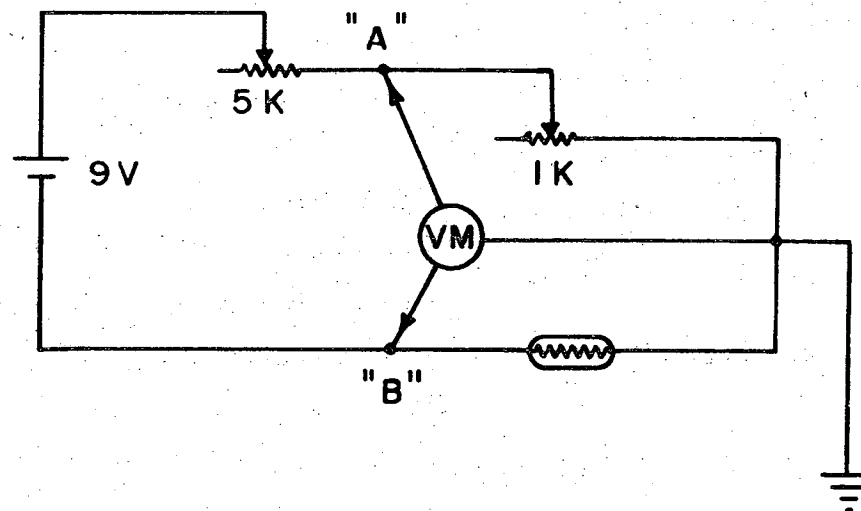
sample was then taken up with a glass-tipped polyethylene micro-pipette which was inserted in a micro-manipulator for transfer to the left thermistor. It was necessary to perform this delicate and critical operation under a 20 power stereo microscope. To hasten the sample deposition, the thermistor was heated electrically to 70°C. Figure 12 shows the heating circuit which was used.

The 1 K helipot serves as a comparison resistor to the thermistor. By setting it to the resistance value of the thermistor at 70°C, which has been measured previously, and adjusting the 5K helipot until the reading on the volt meter in position "A" is the same as that in position "B", the temperature of the thermistor is set to 70°C. Note that since the resistance of the thermistor varies with its temperature, setting it to 70°C requires changing the power applied to it. Varying the 5K helipot does this, with the residual resistance of the helipot serving as a ballast resistance to prevent overheating the thermistor. This operation was always done by reducing the resistance of the 5K helipot from its maximum so that the temperature of the thermistor never exceeded 70°C.

Before insertion into the calorimeter, the thermistor mount was placed in a vacuum desiccator and the house vacuum was applied as a preliminary degassing operation.

D. Operation of Calorimeter

The protective aluminum cap was screwed on the thermistor mount and the mount was plugged into the calorimeter. The outer copper vessel was screwed on and the entire assembly lowered into the constant temperature bath. A mechanical pump was used to evacuate the system. Several Torr of helium were let into the calorimeter in order to hasten



XBL718 - 4043

Fig. 12. Circuit diagram of apparatus used to heat thermistor as sample is deposited.

thermal equilibrium with the constant temperature bath. Three minutes after the helium was admitted, the thermistor heating circuit was connected to both thermistors, the amplitude of the audio oscillator set at 70. After five minutes of heating (eight minutes after the helium was admitted) the helium was pumped out and the amplitude of the audio oscillator was reduced to 40. This amplitude corresponds to a higher temperature of the thermistors than does an amplitude of 70 in the presence of helium. The diffusion pump was used to evacuate the calorimeter vessel to below 10^{-6} Torr. At this point the current and voltage through the left thermistor were measured and its resistance calculated to verify that it was still intact. Four or five minutes after the helium was pumped out (nine or ten minutes of heating) the heating circuit was disconnected. After one minute the calorimeter bridge was turned on to the least sensitive setting, 1/100 battery voltage, and gradually increased to the 1/3 battery setting, with adjustments made on the helipot as necessary to keep the Speedomax recorder on scale. Typically, fifteen to eighteen minutes from the time that the thermistor mount was put in place were required for the calorimeter to reach equilibrium and permit measurement of the heat produced by the isomer in its decay.

The measurement was continued for at least two hours, at which point the sample had decayed sufficiently that a straight base line could be determined. Then the calibration was made and the resistance of the thermistor was measured, as described in Sec. IID.

E. Determination of Yield

The chemical yield of uranium from the sample preparation procedure was determined by a tracer technique. Uranium-232 was selected

because its principal alpha decay mode, at 5.32 MeV, is greater in energy than that of plutonium-239 at 5.15 MeV. Thus an accurate determination of uranium-232 is possible without interference from the lower energy "tail" of the plutonium-239 which is a contaminant of the sample. The sample was completely removed from the bead with dilute HNO_3 and placed on a 1 inch platinum plate for alpha counting. Alpha counting was done with a silicon surface barrier alpha detector and analyzed by a four hundred channel pulse height analyzer, RIDL 3412B. Standard plates of a known aliquot of the tracer solution were prepared such that the counting rate of the standard plate was approximately the same as that of the sample to which it was compared. Counts of standard and sample plates were of ten hours duration.

Peak heights of the principal uranium-232 peak at 5.32 MeV were compared for the chemical yield of uranium. Minor corrections (less than 10%) for the contributions of the neighboring thorium-228 peaks were required for the assay plates. This correction was not required for the sample plates, since the thorium-228 present in the tracer as a decay product is not extracted with uranium by the ether in large enough amounts to interfere.

The amount of uranium-235m actually present during the period of measurement in the calorimeter was calculated by multiplying the amount of uranium-235m present in the plutonium stock solution by this chemical yield factor, and correcting for the decay of the isomer during preparation of the sample.

Immediately after each experiment another ether extraction was done on the plutonium stock solution to remove any uranium-232 tracer that may have remained after the two ether extractions used to obtain

the sample. The three extractions removed over 99% of the tracer. The uranium-235m was allowed to grow into the stock solution overnight.

Hence, the initial amount of the isomer present in the stock solution at the beginning of the experiment was taken as the equilibrium value.

V. RESULTS AND DISCUSSION

A. Introduction

The data from the calorimeter was in the form of a trace of power versus time recorded as the experiment was in progress by the Speedomax recorder. The points were then replotted on linear graph paper to compress the time scale. A straight line would be anticipated in the absence of a sample on the left thermistor, but this was not the case. Rather, a straight baseline was obtained only after a sharp initial curve which was not exactly duplicated from run to run. Thus a simple subtraction of the curve obtained without a sample from the curve obtained with a sample in place was not possible.

The successful analysis of the data was due to the observation that the sharp initial curve was exponential in form. Once it was recognized that the half life of this exponential was nearly the same from run to run for a given set of thermistors in a mount, the analysis of the data became quite straightforward. Thus, when the straight baseline value (which is a function of the setting on the 20K Ω helipot) was subtracted from the data obtained with a sample of uranium-235m on the left thermistor the curve which remained was a composite curve of the 26.5 minute half life isomer and the shorter half life thermistor curve. This composite curve was then analyzed in the same way as a radioactive decay curve involving two components.

The half lives of thermistor sets tested in the calorimeter ranged from four to eleven minutes. Since the energy dissipated in the sample-holding thermistor by the uranium-235m decays with a 26.5 minute half life, the thermistor sets chosen for these runs were those with the

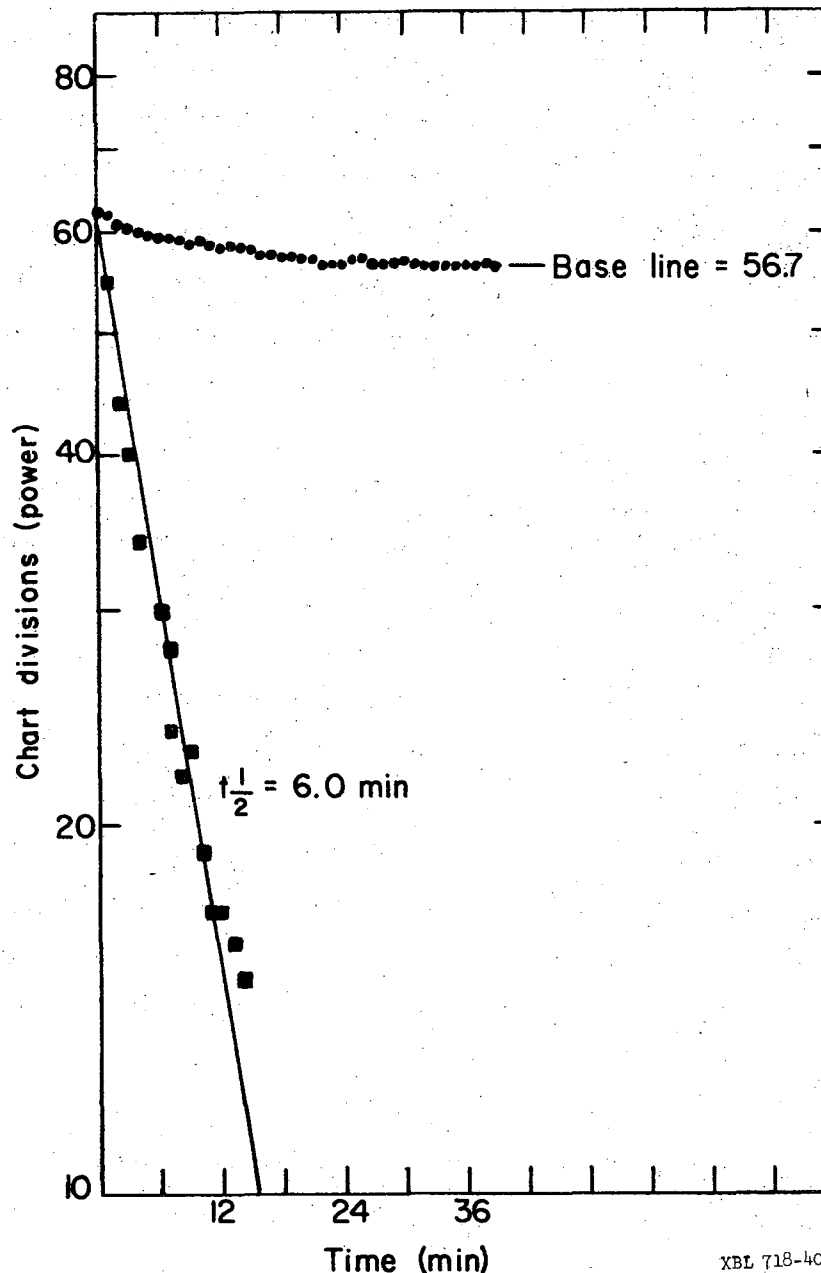
shortest characteristic lifetimes in order to avoid any ambiguity in the interpretation of the data.

Some further restrictions were placed on the experiment. The set of thermistors used in a measurement was required to show the same characteristic half life before the sample was placed on the left thermistor during the measurement, and after the activity of the isomer had decayed away. This provided assurance that the thermistor set (and the rest of the system, as well) was performing properly at all times.

B. Uranium-235m Runs

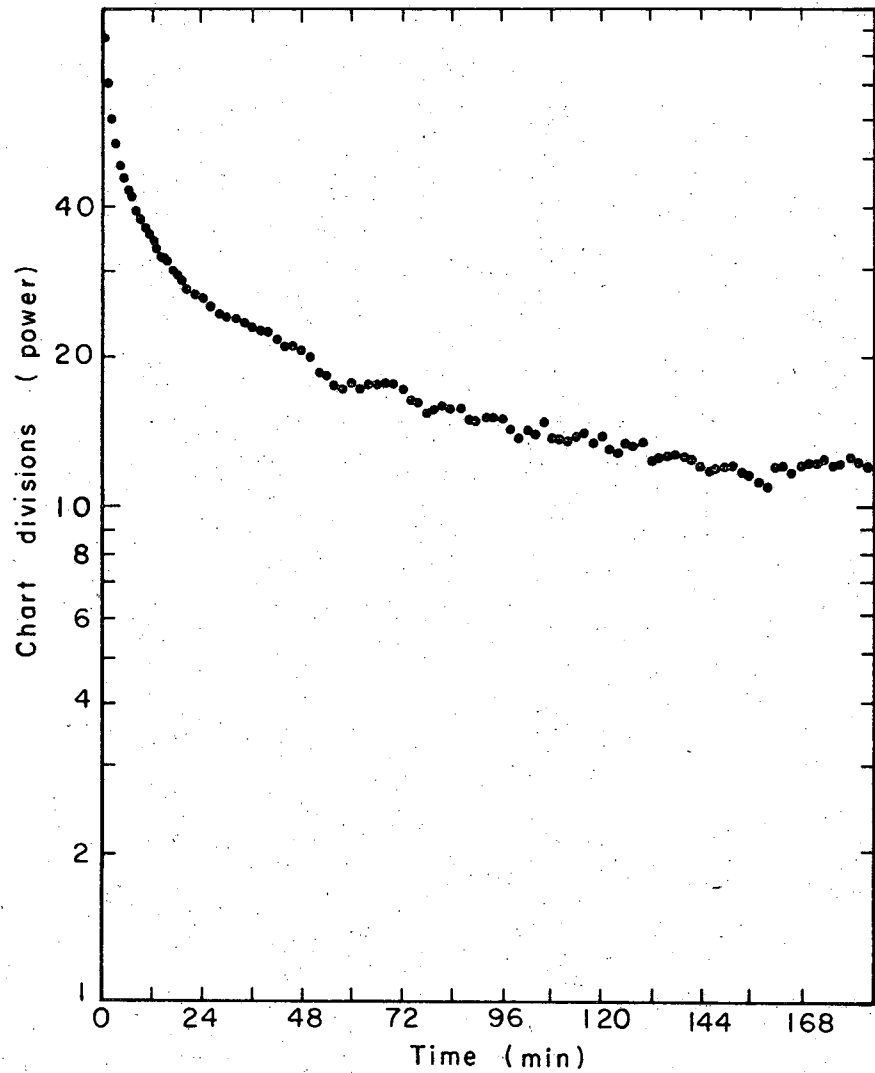
The data from two uranium-235m measurements are presented in the following figures and tables. In Figs. 13, 15, 16, 18, 21, and 23, the ■ points are multiplied by 10.

Figure 13 shows the behavior of the thermistor set used in Run #1 before the actual run. Note the half life of six minutes, obtained by subtracting the baseline of 56.7 from the rest of the curve. The data from the first uranium-235m run is shown in Fig. 14. In Fig. 15 a smooth curve has been drawn from the points in Fig. 14, and the baseline of 12.5 has been subtracted from this curve to give a second curve, which is represented by the solid points. This is the composite curve of the isomer's decay and characteristic behavior of the thermistor set. The lower portion of this curve is seen to be a straight line with a half life of 26.5 minutes; this represents the power dissipated in the thermistor bead by the decay of the uranium-235m. When the values of this line extrapolated back to time 0 on the chart are subtracted from the first part of the curve, another straight line is obtained. The half life of this line is four minutes, close to the value of six minutes



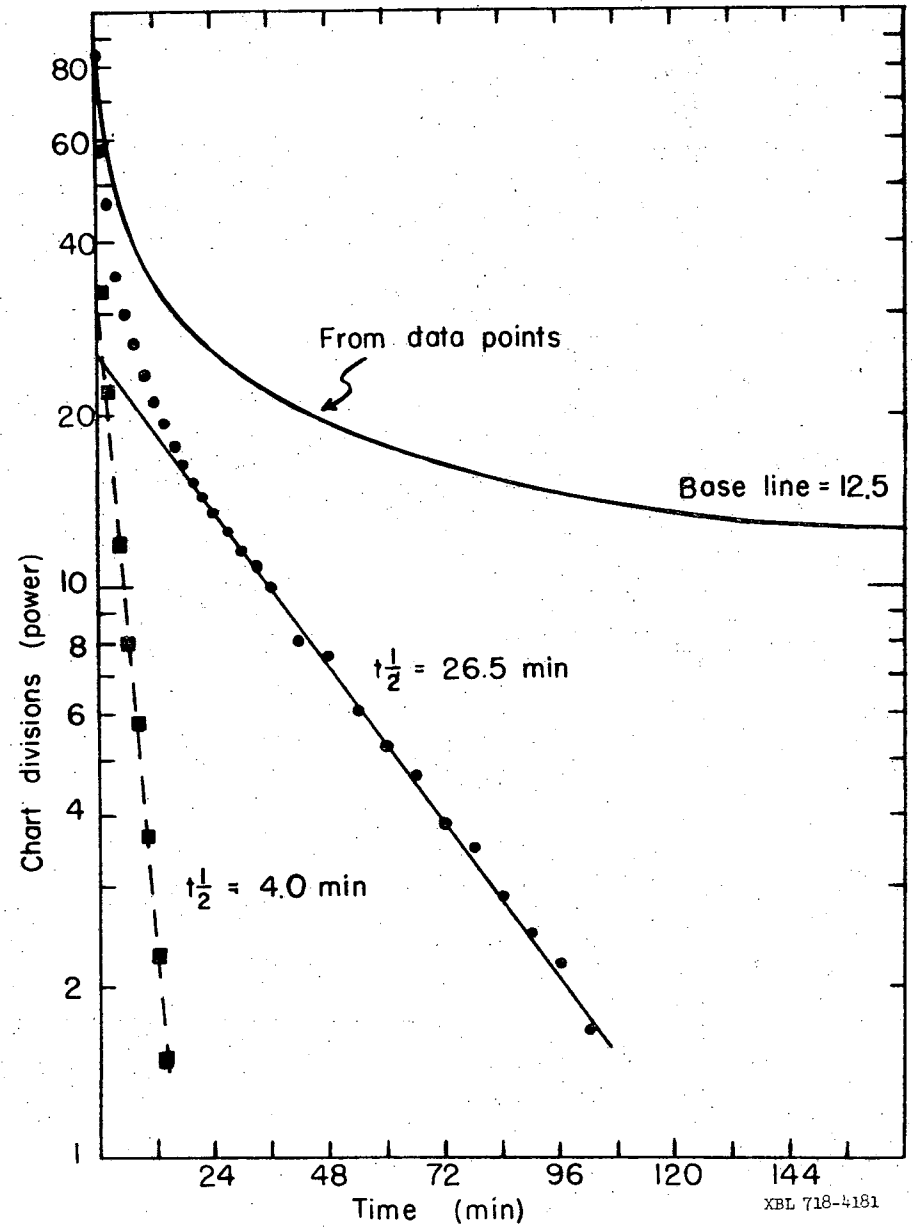
XBL 718-4080

Fig. 13. Behavior of thermistor set before uranium 235-m run #1.



XBL718-4064

Fig. 14. Data from uranium 235-m run #1.



XBL 718-4181

Fig. 15. Analysis of data from uranium 235-m run #1.

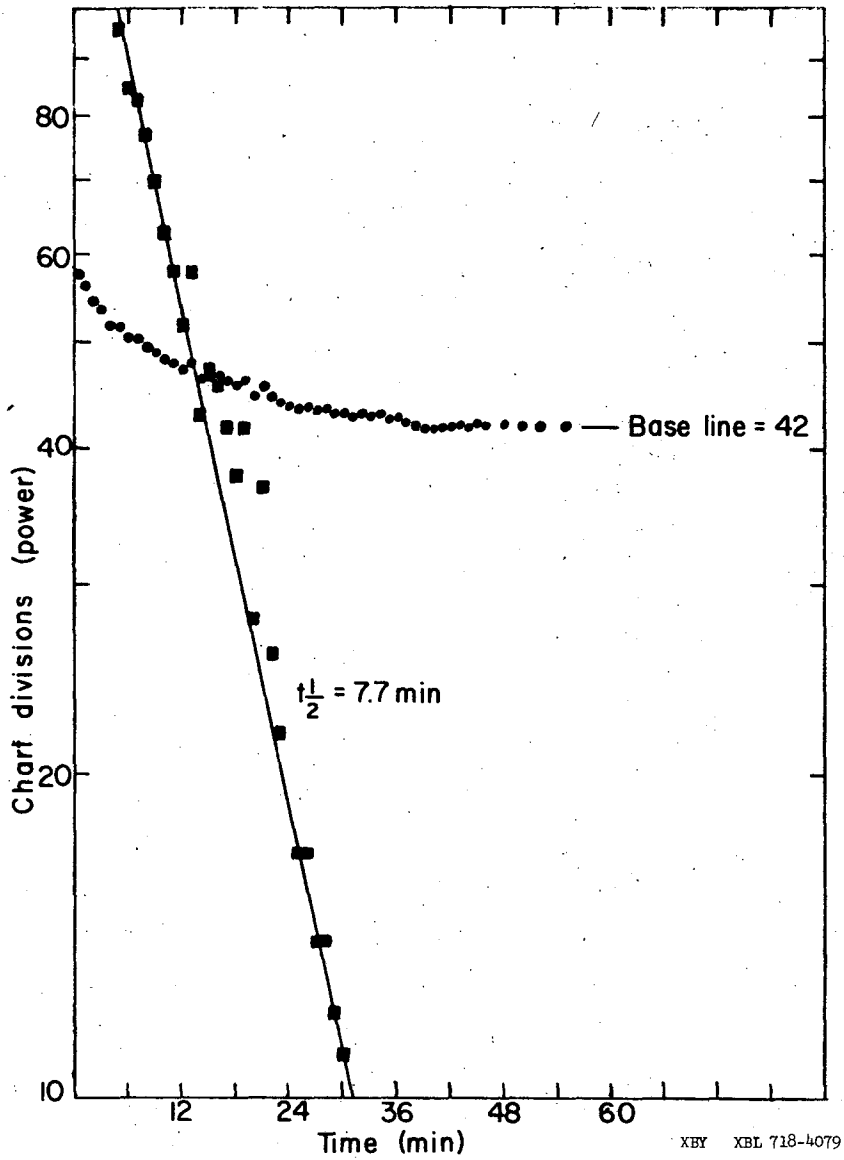
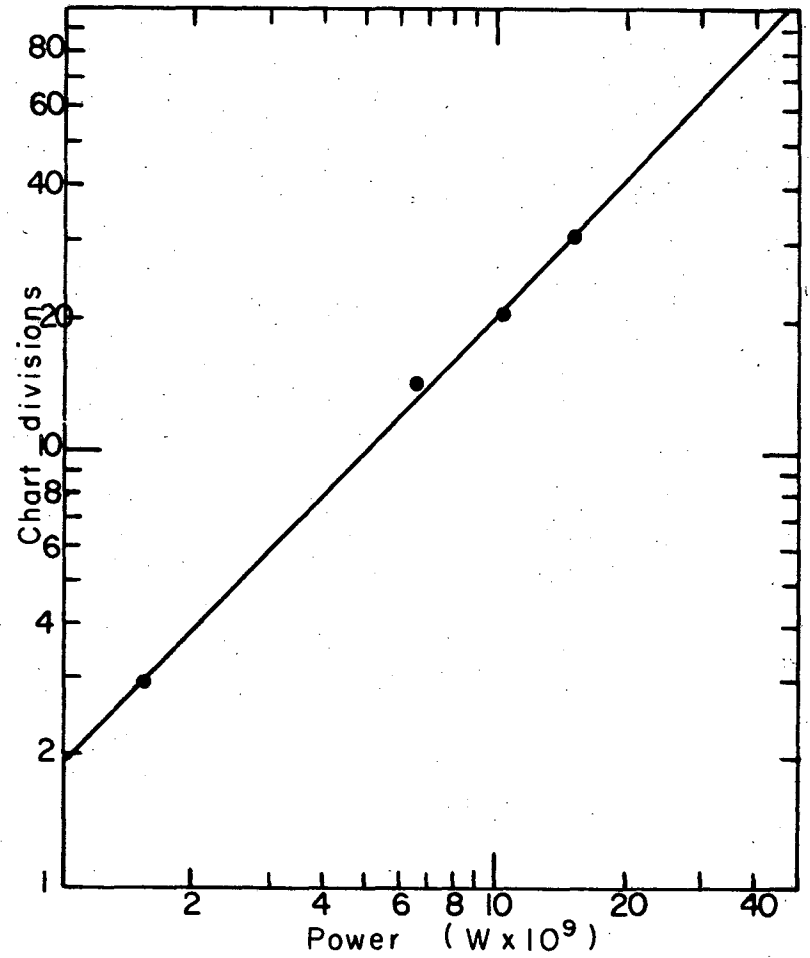


Fig. 16. Behavior of thermistor set after uranium 235-m run #1.



XBL718-4072

Fig. 17. Calibration of calorimeter for uranium-235m run #1.

previously obtained for the characteristic half life of the thermistor set. Figure 16 shows the behavior of the same thermistor set with the sample of uranium still in place, but after a sufficient time has elapsed so that the isomer has decayed away completely. Note that there is no 26.5 minute component. When the baseline of 42 is subtracted from the curve, a straight line results, a simple exponential with a half life of 7.7 minutes.

In Fig. 17 is shown the calibration of the calorimeter. Each chart division (the abscissa in Figs. 13-16) thus represents 4.9×10^{-10} watt or 3.06×10^9 eV/sec.

The calculation of the decay energy of uranium-235m proceeds as follows:

The ether extraction was made from 10.9 g of plutonium-239. The number of atoms of plutonium-239 was thus

$$\frac{(10.9)(6.023 \times 10^{23})}{239} = 2.74 \times 10^{22}$$

Since the half life of plutonium 239 is much longer than that of uranium-235m, and since the uranium was allowed to grow into the stock solution for an interval very long compared with the half life of the uranium-235m,

$$d/\text{sec}(\text{Pu}239) = d/\text{sec}(\text{U}235\text{m})$$

at time $t = 0$ (when the separation from the plutonium is completed).

$$d/\text{sec}(\text{Pu}239) = (N\lambda)\text{Pu}239 = \frac{(0.693)(2.74 \times 10^{22})}{(3.16 \times 10^7)(2.44 \times 10^4)}$$

$$= 2.47 \times 10^{10} \text{ d/sec}(\text{U}235\text{m}) \text{ at time } t = 0$$

The graphs of Figs. 14 and 15 begin 139 minutes after extraction was completed. Taking 26.5 minutes as the best value of the half life of the decay, six half lives, or 159 minutes, will have elapsed at $t = 20$ minutes on the graphs.

The chemical yield was determined by the use of ^{232}U , as described earlier, and was 22.6%.

The disintegration rate of the $^{235\text{m}}\text{U}$ at $t = 159$ minutes (20 minutes, chart time) is found by multiplying the original number of disintegrations of the isomer per second, 2.47×10^{10} , by the chemical yield and by 1/64 to correct for the six half lives which have elapsed since the separation of the $^{235\text{m}}\text{U}$ from the ^{239}Pu stock.

$$(2.47 \times 10^{10})(0.226)(1/64) = 8.72 \times 10^7 \text{ d/sec}$$

The solid points in Fig. 15 represent the 26.5-minute half life component. At chart time=20 minutes the power intercept is seen to be 15 chart divisions.

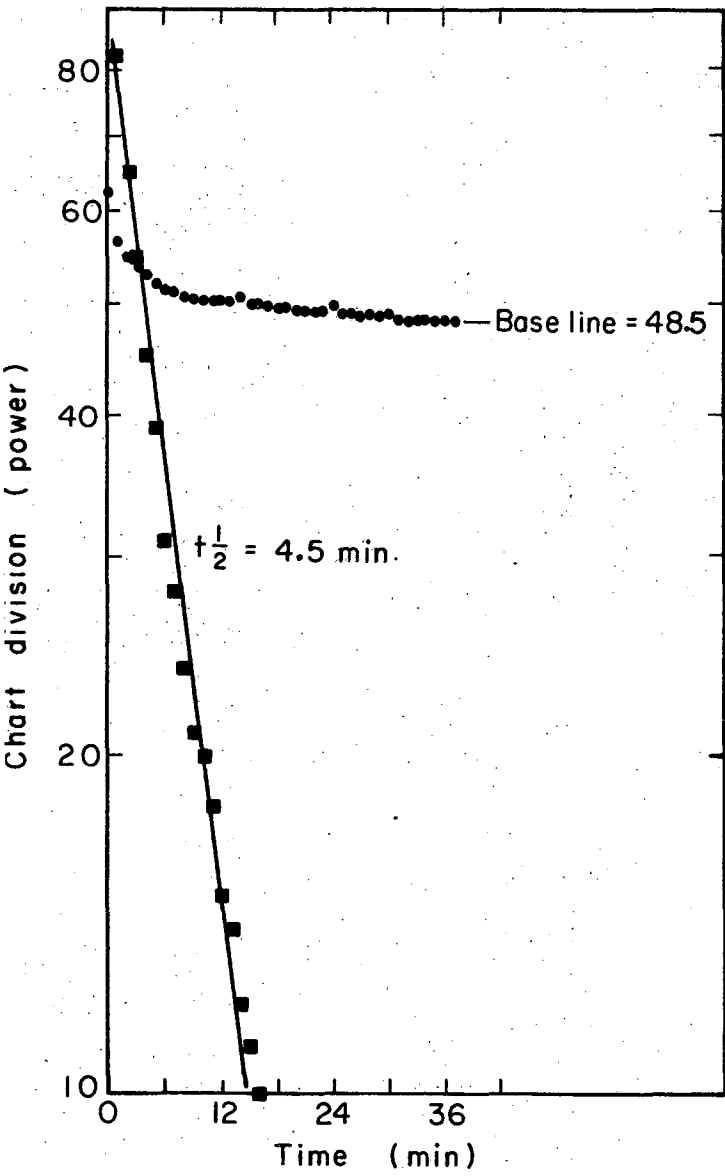
It has been previously calculated from Fig. 17 that each chart division represents 3.06×10^9 eV/sec. Thus the power corresponding to

$$(15)(3.06 \times 10^9) = 45.9 \times 10^9 \text{ eV/sec}$$

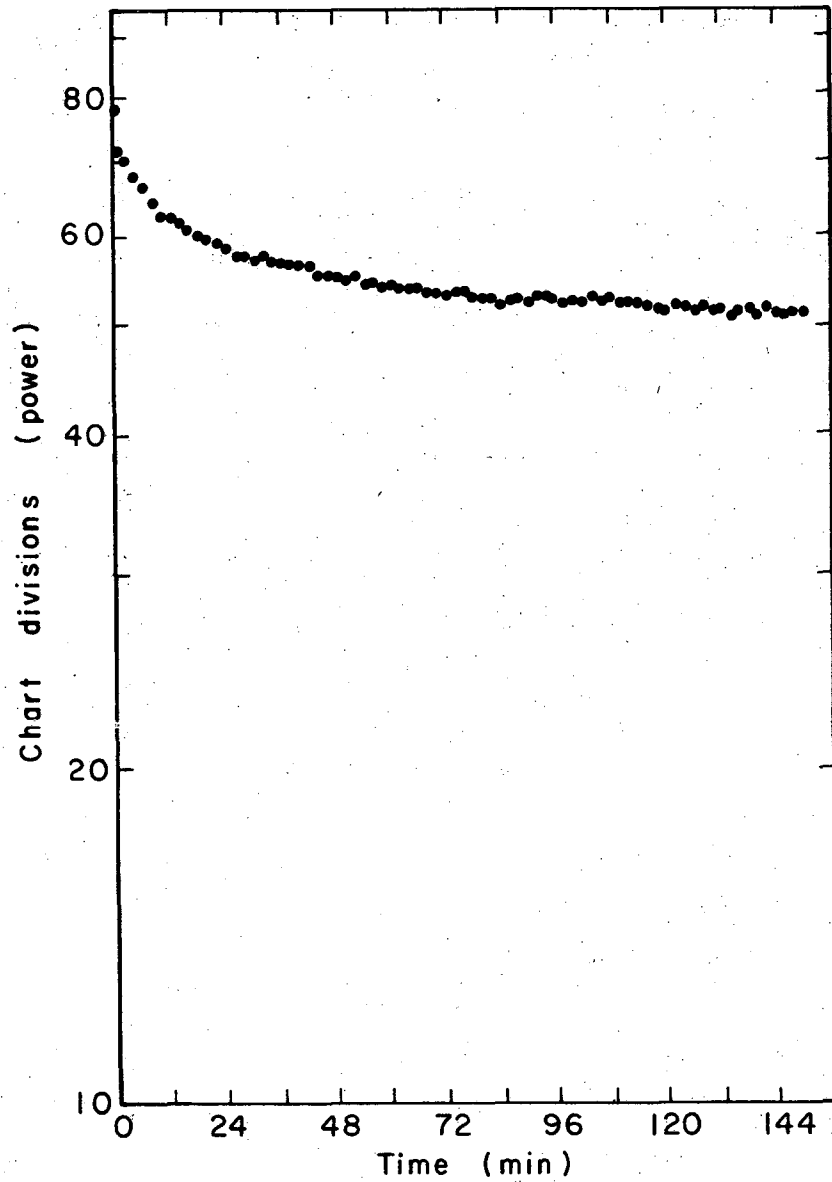
The number of disintegrations occurring at this time has been calculated above to be 8.72×10^7 d/sec. Therefore each decay dissipates

$$\frac{45.9 \times 10^9 \text{ eV/sec}}{8.72 \times 10^7 \text{ d/sec}} = \underline{526 \text{ eV/decay}}$$

The data from Run #2 may be analyzed in a similar manner. Figure 18 shows the behavior of the thermistor set prior to the run; Fig. 19

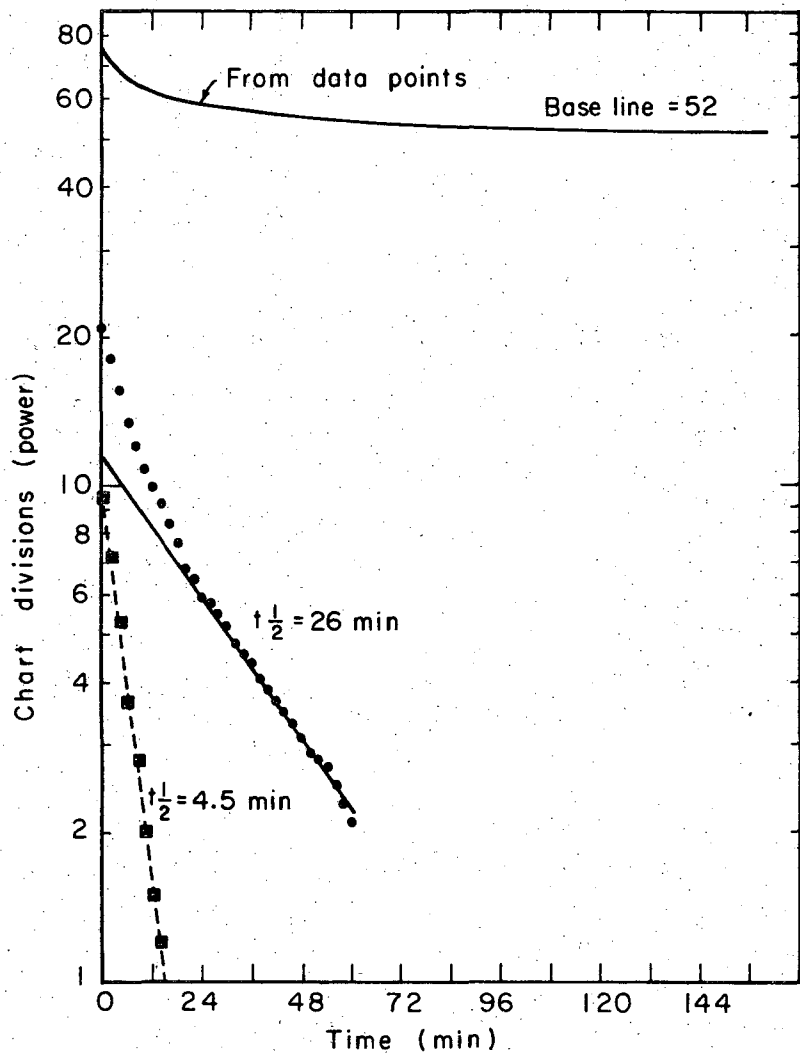


XBL718-4071



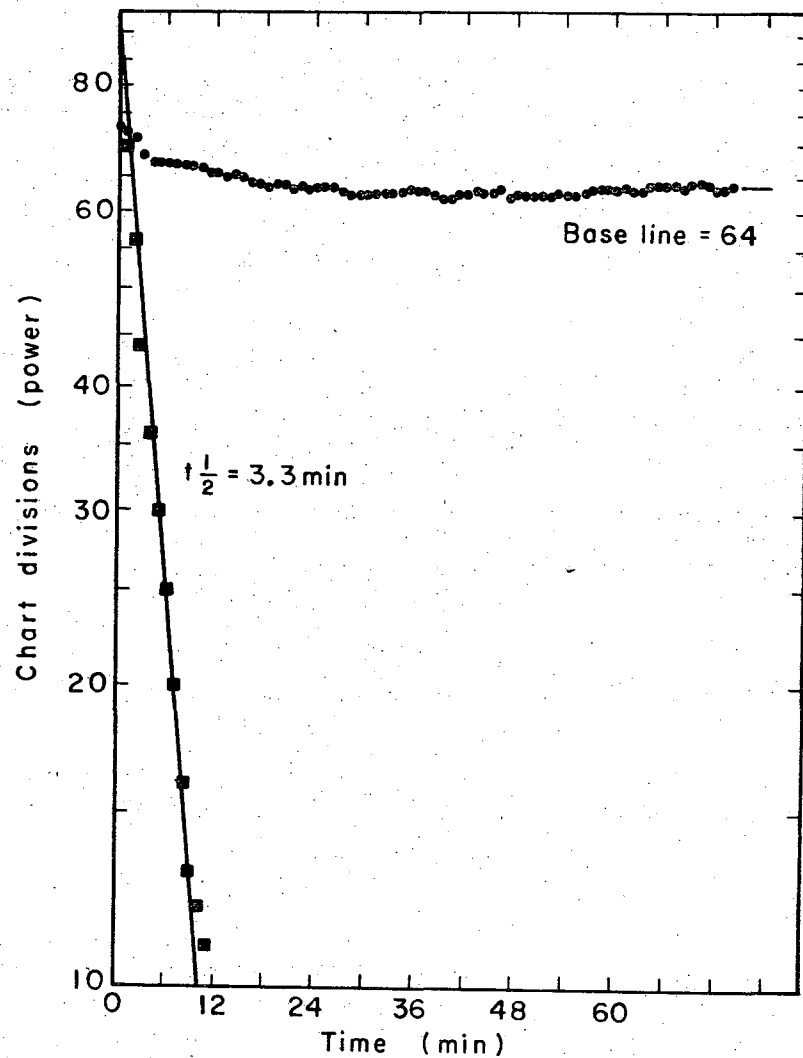
XBL718-4069

Fig. 19. Data from uranium 235-m run #2.



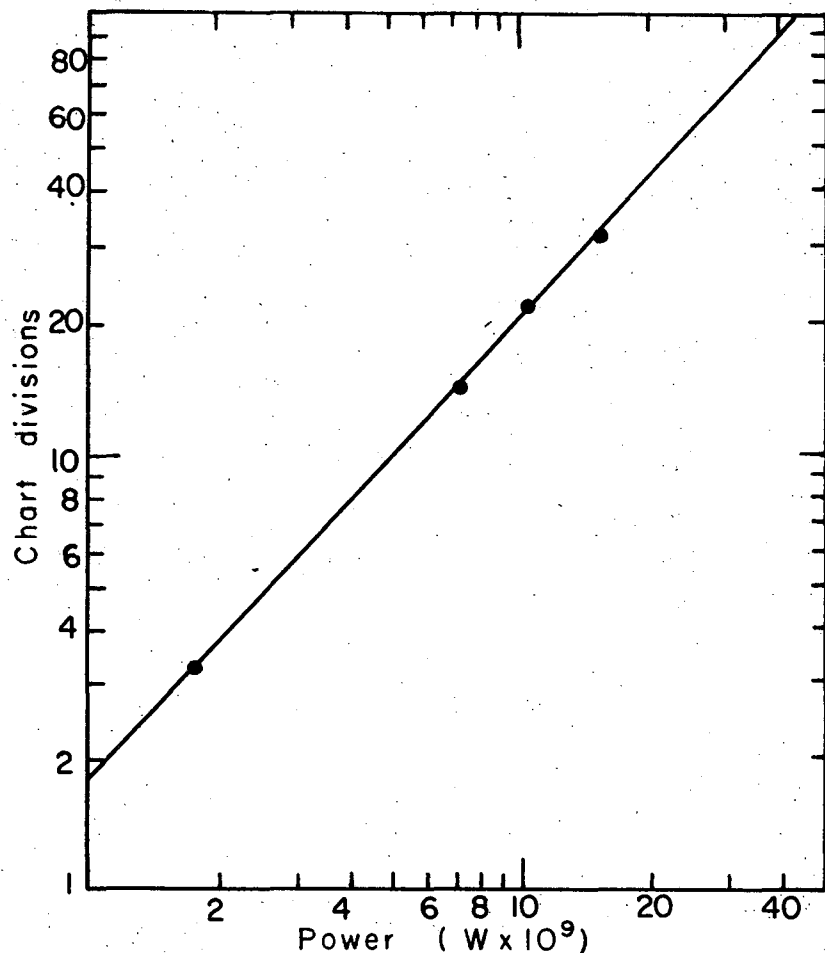
XBL718-4074

Fig. 20. Analysis of data from uranium 235-m run #2.



XBL718-4066

Fig. 21. Behavior of thermistor set after uranium 235-m run #2.



XBL718-4070

Fig. 22. Calibration of calorimeter for uranium-235m run #2.

shows the data from the run. The data are analyzed in Fig. 20; and Fig. 21 shows the behavior of the thermistor set after the run, with the sample still in place.

The ether extraction for this run was made from 9.9 grams of plutonium-239, or

$$\frac{(9.9)(6.023 \times 10^{23})}{239} = 2.50 \times 10^{22} \text{ atoms of } {}^{239}\text{Pu}$$

At time $t = 0$,

$$d/\text{sec}(\text{Pu239}) = d/\text{sec}(\text{U235m}) = (N\lambda)\text{Pu239}$$

$$= \frac{(0.693)(2.50 \times 10^{22})}{(3.16 \times 10^7)(2.44 \times 10^4)} = 2.25 \times 10^{10} \text{ d/sec}(\text{U235m})$$

The graphs of Figs. 19 and 20 begin 152 minutes after the separation was completed (time $t = 0$). Thus, six half lives (159 minutes) have elapsed at $t = 7$ minutes on the graph.

The disintegration rate of ${}^{235\text{m}}\text{U}$ at $t = 7$ minutes, graph time, is found by multiplying the disintegration rate at $t = 0$, calculated above, by the chemical yield, which was 13.5%, and by $1/64$.

$$(2.25 \times 10^{10})(0.135)(1/64) = 4.75 \times 10^7 \text{ d/sec}$$

At $t = 7$ minutes, graph time, the power intercept of the 26-minute component (the straight line drawn from the solid points) is 9.5 chart divisions.

Figure 22, the calibration of the calorimeter, indicates that each chart division corresponds to 4.95×10^{-9} watt, or 3.09×10^9 eV/sec.

At seven minutes, graph time,

$$(9.5)(3.09 \times 10^9) = 29.3 \times 10^9 \text{ eV/sec}$$

is being dissipated in the thermistor by 4.75×10^7 d/sec. The decay energy is thus:

$$\frac{29.3 \times 10^9 \text{ eV/sec}}{4.75 \times 10^7 \text{ d/sec}} = \underline{617 \text{ eV/decay}}$$

The mean value for the decay energy of uranium-235m is

$$(572 \pm 33) \text{ eV}$$

where 33 eV is the standard deviation of the mean.

The two types of errors are involved in the measurement: random and systematic. In the class of random errors are the precision of the assaying techniques used and the accuracy with which the preparation time was measured. Two assays are performed in the course of sample preparation: one to determine the amount of plutonium-239 from which the extraction was made, the other to measure the aliquot of uranium-232 used as the tracer. The more difficult and involved of the two was the assay of the plutonium-239 stock solution, because it required a primary aliquot of 10λ, a dilution in a volumetric flask, and then a second aliquot which was placed on a platinum plate for counting. In addition, this procedure was necessarily performed in a gloved box, which further compounded the difficulty of the operation. To measure the practical limit of precision of this assay, nine assays were made over a two day period. The fractional standard deviation of the results was 0.9%.

The measurement of the 100λ aliquot of the uranium-232 placed in the plutonium-239 stock solution was a much less difficult operation, since it involved only one aliquot, and was performed in a hood rather than the gloved box. The major uncertainty involved in the uranium-232 assay is that associated with the interpretation of the alpha particle spectrum. As previously noted in Sec. IV E, a correction must be made for the presence of neighboring thorium-228 peaks. The overall error introduced in the uranium-232 assay was estimated at not over 10%.

The alpha counters used in the experiment were checked with standard sources of known activity to determine geometry factors; and a Chi-square test applied to the data indicated that they were functioning properly. The error introduced by the counters is included in the assay error estimates.

The measurement of sample preparation time and chart time was done by a standard electric clock. The main difficulty here was in deciding upon time $t = 0$, the moment when the second ether extraction of the plutonium-239 stock was completed. When the shaking was stopped, about half a minute passed before the ether and the plutonium-239 solution separated into two distinct phases, during which time some uranium was still being extracted, although to a lesser extent than during agitation. An uncertainty of ±30 seconds introduces an error of ±1%.

The statistically combined effect of these uncertainties is 10.1%. This estimate of the error in a single measurement leads to a standard deviation of the mean of 7.1%, which is in good agreement with that calculated directly from the measured values of the decay energy,

$$(572 \pm 33) \text{ eV or}$$

$$572 \pm 5.8\%$$

The possible systematic errors in the measurement--errors of constant magnitude which recur during each run--are more difficult to evaluate. The limits of accuracy of the numbers for the half lives of Pu-239 and U-235m are sources of systematic error. The half life of Pu-239 is known quite accurately. The half life of U-235m has been reported as 26.5 ± 0.2 minutes,³ 26.6 ± 0.3 minutes,⁴ and 26.16 ± 0.03 minutes.⁶ The half life used in the calculation was 26.5 minutes. If 26.16 minutes is chosen instead, the values obtained for the energy would be 5.7% greater.

The most serious possible systematic error would be some unknown bias in the calorimeter itself which would lead to a faulty calibration of the instrument. Section II D, Calibration, describes the precautions taken to insure the accuracy and suitability of the calibration.

Even so, it would be desirable to use the calorimeter to measure the decay energy of a known transition in order to eliminate the possibility of a significant systematic error in the instrument. There are no other similar low energy, highly converted gamma transitions whose energy is known. Beta transitions are too high in energy for the necessary qualification that virtually all the transition energy be dissipated within the sample.

C. Bismuth-212 Run

Of the very few alpha emitters with suitable half lives, bismuth-212 with a half life of 60.5 minutes is easily prepared from thorium-228. 10^7 to 10^8 d/m of thorium-228 were placed on a cation exchange resin in 0.1 M HCl. Elution of lead-212 and bismuth-212 proceeded with 2 M HCl. The lead-212 was eluted first and discarded, since its 10.6 hour half

life is too long for the calorimetric measurement. The bismuth-212 sample, which was free of all detectable lead-212, was taken from the column and placed directly onto a thermistor bead. The calorimeter was operated in the standard manner to obtain a power vs time curve as in the uranium-235 runs. The interpretation of this curve was not as straightforward as in the uranium-235m measurement for two reasons. First, only 36% of the bismuth-212 decays by alpha emission; the remaining 64% decays by beta emission to polonium-212, which then decays by alpha emission with a 304 ns half life. Since the energies of these two alpha transitions are different, an average alpha energy must be used in the calculation. If the alpha particle energies are multiplied by their respective percentages and added, an average alpha energy of 7.9 MeV is obtained. The exceedingly short half life of the polonium-212 means that its alpha decay will proceed with the half life of the parent bismuth-212, so no half life correction is necessary.

Secondly, not all the alpha particles are absorbed within the sample. This factor is difficult to evaluate with precision, but an estimate may be made. The range of a 7.9 MeV alpha particle in air is 75 mm. Using the Bragg-Kleeman rule,

$$R = 3.2 \times 10^{-4} \frac{\sqrt{A_1}}{\rho_1} R_{\text{air}}$$

and values of 50 for the atomic mass, A_1 , of the thermistor and 3 for its density, ρ_1 , the range of an alpha particle in the thermistor bead is calculated to be 0.056 mm. The bead is an ellipsoid whose minor axis is 0.41 mm, or over 7 times the range of a 7.9 MeV alpha particle. In a crude analysis, then, slightly under half the alpha particle energy will

be dissipated within the bead, assuming an isotropic distribution of alpha particles. In addition, there is some mass associated with the sample, and this has the effect of increasing the number of alpha particles absorbed within the bead and sample. It was impossible to measure the amount of this mass, except to note that it was distributed fairly evenly over the whole head and was about 0.02 mm thick. It seems reasonable, then, to assume that between 50% and 75% of the total alpha particle energy is detected by the calorimeter.

The data from the bismuth-212 run are presented in the same way as that from the uranium-235m runs. Figure 23 shows the behavior of the thermistor set before the run. The characteristic half life of the set is eleven minutes. Figure 24 shows the data from the bismuth-212 run, and Fig. 25 shows the analysis of these points.

The straight baseline has not quite been reached, due to the necessity of removing the sample from the thermistor bead while there is still sufficient bismuth-212 alpha activity to be counted for the yield determination. The following reasoning was used in determining the eventual baseline of 25. Utilizing that portion of the curve after the initial short half life associated with the thermistors has disappeared, it may be seen that in the interval between 120 minutes and 180 minutes (about one half life) the curve has dropped three divisions to 28.0. In the interval between 180 minutes and 240 minutes, it will drop 1-1/2 divisions to 26.5, and so forth, converging to a series limit of 25.0. The curve which results from subtracting the baseline of 25.0 from the data curve is represented by the solid points. This line may be resolved into two components, one with a half life of 60.5 minutes, which is exactly the half life of the bismuth-212 alpha decay. The shorter

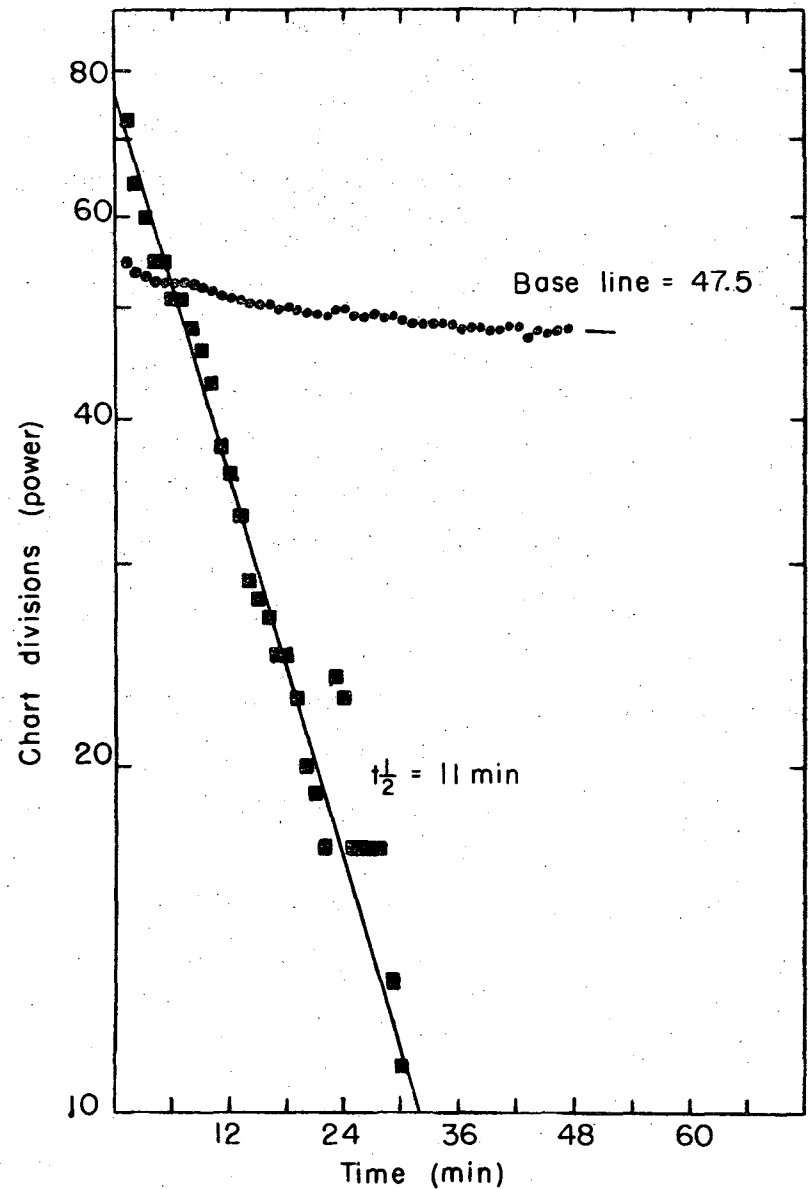
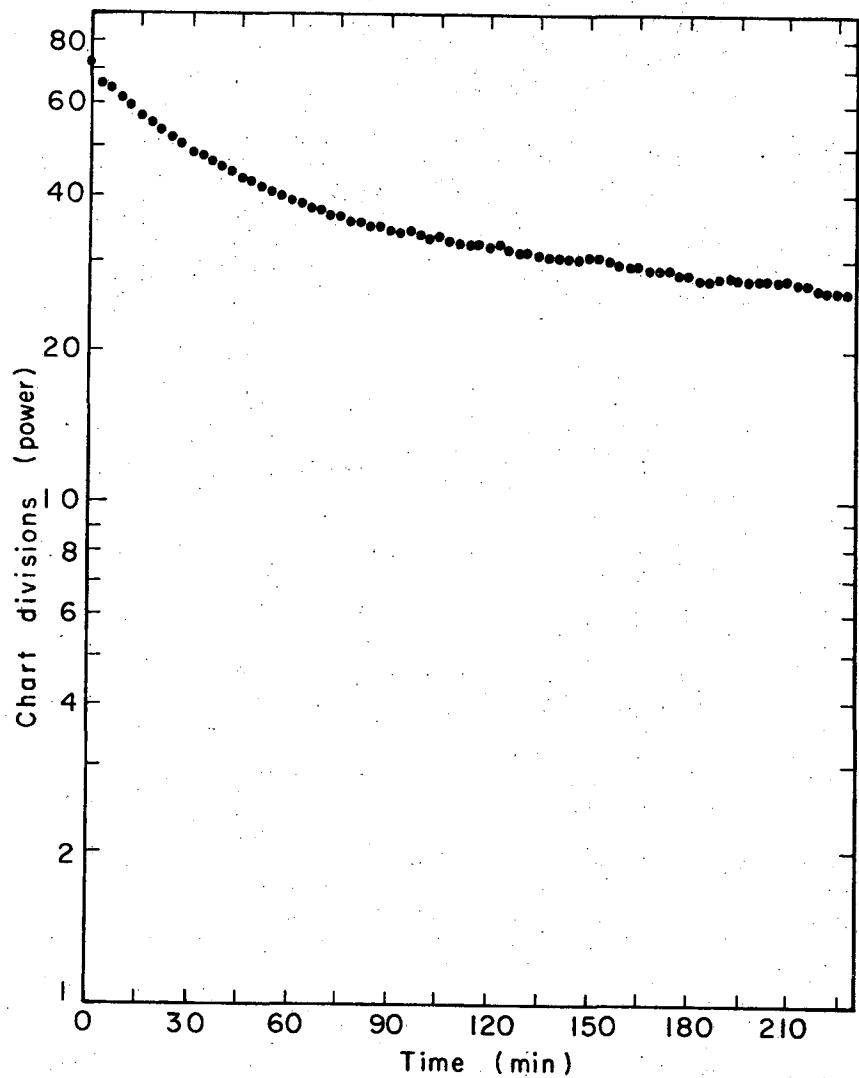
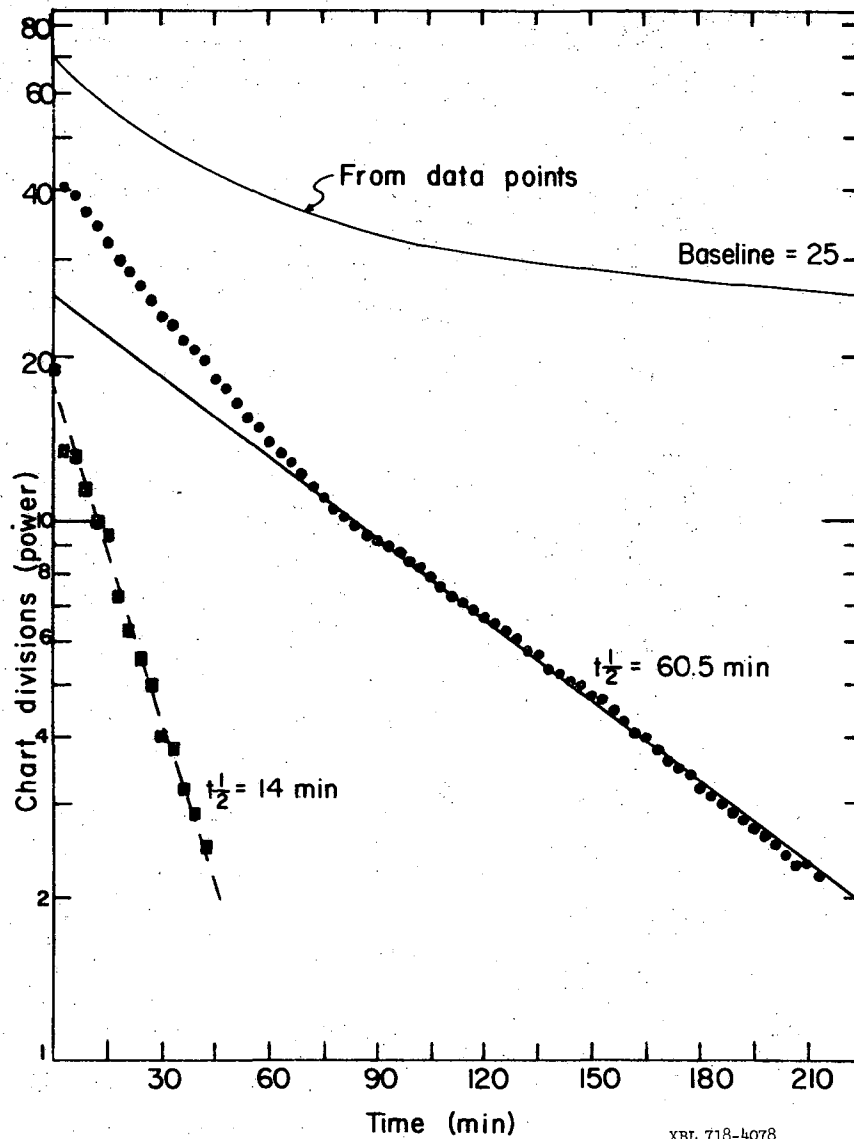


Fig. 23. Behavior of thermistor set before bismuth-212 run.



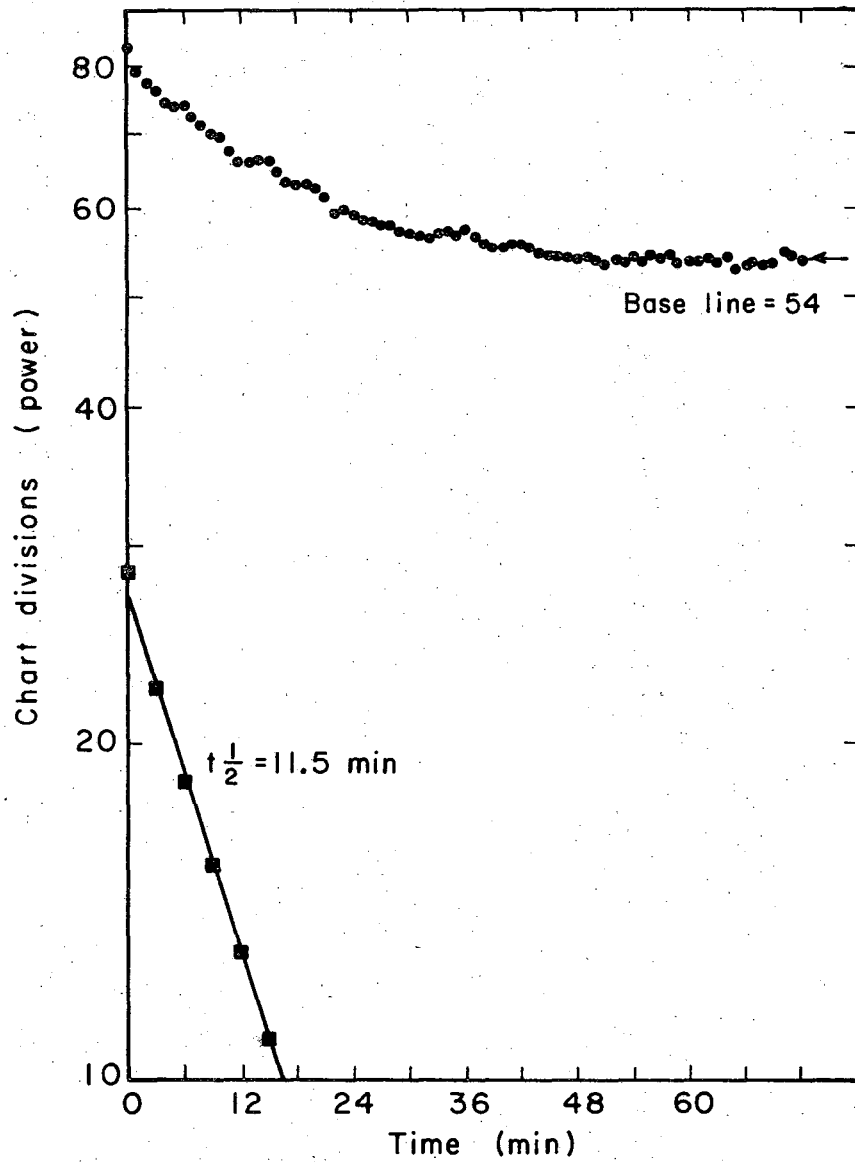
XBL718-4065

Fig. 24. Data from bismuth-212 run.



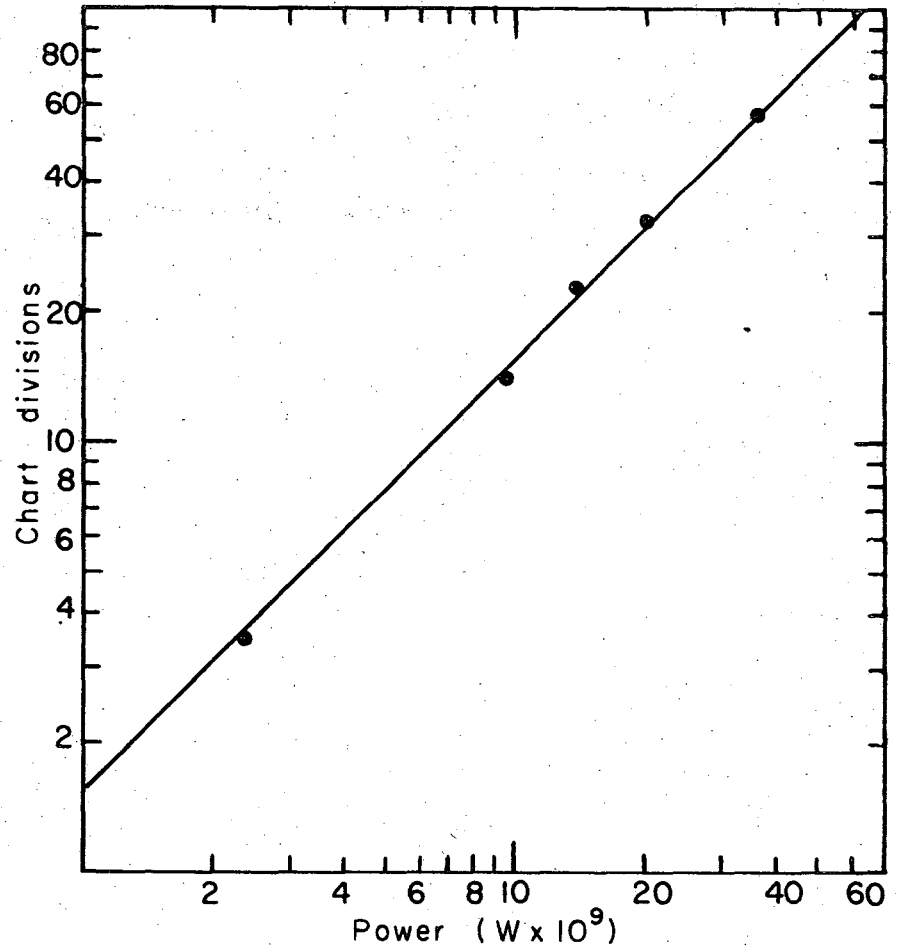
XBL 718-4078

Fig. 25. Analysis of data from bismuth-212 run.



XBL718-4068

Fig. 26. Behavior of thermistor set after bismuth-212 run.



XBL718-4073

Fig. 27. Calibration of calorimeter for bismuth-212 run.

component has a half life of 14 minutes, which is close to the eleven minute half life previously noted for the thermistor set.

Figure 26 shows the behavior of the set after the bismuth-212 run. The half life is 11.5 minutes.

The analysis of the data of the bismuth-212 run proceeds as follows:

The bismuth-212 and polonium-212 activities were removed from the bead and counted at 4:11, P.M.* The counting rate was 24,049 c/m. The alpha counter used had a geometry factor of 51.5%, so the disintegration rate was

$$\frac{2.40 \times 10^4 \text{ c/m}}{(0.515)(60 \text{ sec/min})} = 7.77 \times 10^2 \text{ d/sec at 4:11, P.M.}$$

Four half lives, or 4 hours, 2 minutes, earlier (12:09, P.M.) the disintegration rate was

$$(7.77 \times 10^2 \text{ d/sec})(16) = 1.24 \times 10^4 \text{ d/sec}$$

Assuming 7.9 MeV per alpha decay, the energy dissipated in the thermistor bead at 12:09, P.M., is

$$(1.24 \times 10^4 \text{ d/sec})(7.9 \text{ MeV/d}) = 9.8 \times 10^4 \text{ MeV/sec}$$

From Fig. 27, the calibration of the calorimeter, it may be seen that one chart division corresponds to 6.4×10^{-10} watt, or 3.99×10^3 MeV/sec. The time $t = 0$ of the chart occurred at 11:26, A.M. 12:09, P.M., then, is 43 minutes into the chart. At $t = 43$ minutes, the power intercept of

the 60.5-minute component was 15.9 divisions, or a power of

$$(15.9 \text{ div.})(3.99 \times 10^3 \text{ MeV/div.}) = 6.33 \times 10^4 \text{ MeV/sec}$$

At 12:09, P.M., then, 6.33×10^4 MeV/sec was being dissipated in the thermistor bead. As calculated above, 9.8×10^4 MeV/sec was being produced by the decay at 12:09. However, it was previously estimated that only 50% to 75% of the power produced by the decay is actually being absorbed within the thermistor and detected by the instrument. Therefore, between 4.9×10^4 MeV/sec and 7.3×10^4 MeV/sec would be expected to be detected by the calorimeter. The answer obtained, namely 6.33×10^4 MeV/sec is within this range. Thus, the likelihood of an unknown systematic error in the uranium-235m measurement is eliminated.

* Clock times are used here in order to simplify the discussion.

VI. ALPHA DECAY HALF LIFE OF THE ISOMER AND COSMOLOGICAL CONSEQUENCES

A. Uranium Cosmochronology

The age of our galaxy has been the subject of much discussion and calculation. One well-established observational technique for determining the age of the galaxy was introduced in 1957 by Burbidge, Burbidge, Fowler, and Hoyle.⁴⁷ Radioactive species of very long half lives, namely uranium-235 and uranium-238, occur naturally. The present abundances of these isotopes in our solar system have been estimated,⁴⁸ and their half lives are known. Thus, the ratio $^{235}\text{U}/^{238}\text{U}$ may be plotted as a function of time. According to the model for nucleosynthesis proposed by Burbidge, et al., now widely accepted, the heaviest elements were formed by a rapid neutron capture process in supernovae, and the production ratio of these two isotopes may be calculated quite simply. The time intercept at which this ratio occurs is taken to be the age of the material in our solar system. The age of the galaxy is then obtained by adding to this number the mean time required for stars to evolve to the supernova stage in which the radioactive nuclei are formed.

Using this method, but assuming a rapid evolution of the star to the supernova stage (10^8 years), Burbidge, et al. obtained 6.6×10^9 years for the age of the elements if they were produced in a single event, or $6.6\text{--}11.5 \times 10^9$ years for a constant rate of element production in the galaxy. In subsequent investigations Fowler and Hoyle⁴⁹ assumed an exponentially-decreasing rate of element synthesis over the lifetime of the galaxy and in addition hypothesized that the stars which evolve to the supernovae require $3\text{--}4 \times 10^9$ years to do so. They calculated the age of the galaxy to be 15×10^9 years. A further refinement by Fowler⁵⁰ and a calculation by Clayton,⁵¹ in which he introduced Re-187

as a chronometer, substantiate this number. Dicke,⁵² on the other hand, assumed a rapid evolution to the supernova stage and a constant rate of element synthesis of 40% of the heavy elements, with 60% being formed in a single event, and obtained a galactic age of 7×10^9 years.

The present ratios of these isotopes and their production ratios are generally accepted quantities. The variation in the values obtained for the age of the galaxy reflects different assumptions concerning the history of the isotopes between their formation and their incorporation into the solar system. Were they formed in one single supernova or were they formed in a continuous series of supernovae occurring between the formation of the galaxy and the condensation of the solar system? Has the galaxy been an autonomous system since its origin or has it acquired new material from intergalactic space at various times?

One other question presents itself in connection with the abundance of uranium-235. As we have seen, the transition energy of the isomeric state is exceedingly low. Might excitation of the isomer occur in the envelopes of stars or in hot portions of interstellar material? And if so, are the nuclear decay properties of the isomer, specifically the half life for alpha decay significantly different from those of the ground state?

B. Coulomb Excitation Calculation

With respect to the first of these questions, interstellar space contains charged particles of high energies which may produce a nuclear transition by Coulomb excitation. Alder, Bohr, Huus, Mottelson, and Winther⁵³ give a Coulomb excitation cross section:

$$\sigma = \sum_{\lambda=1}^{\infty} (\sigma_{E\lambda} + \sigma_{M\lambda})$$

Since the transition from ground state to isomer is an electric octupole transition, the cross section for magnetic excitation, $\sigma_{M\lambda}$, is not used, and only the electric excitation cross section need be considered.

$$\sigma_{E\lambda} = C_E E^{(\lambda-2)} (E-\Delta E')^{(\lambda-1)} B(E\lambda) f_{E\lambda}(\eta_i, \xi)$$

For

$$\lambda = 3, C_E = 9.298 \times 10^2 \left(1 + \frac{A_1}{A_2}\right)^{-4} \frac{A_1}{Z_1^2 Z_2^4} \text{ barns}$$

where: E is the energy of the projectile

$$\Delta E' = \left(1 + \frac{A_1}{A_2}\right)^{-4} \Delta E, \text{ where } \Delta E \text{ is the transition energy}$$

A_1 and A_2 are the masses of the projectile and target nuclei in units of the proton mass; Z_1 and Z_2 are the atomic numbers of projectile and target nuclei; $f_{E\lambda}(\eta_i, \xi)$ measures the effective strength of the interaction. It is obtained from Fig. II4 in Ref. 7; $B(E\lambda)$ is the reduced transition probability for the excitation of the isomer, given in units of $e^2(10^{-24})^\lambda$.

This quantity is best estimated by substituting the experimentally determined values of the half life and transition energy for the $1/2 \rightarrow 7/2$ transition in plutonium-237 into the following equation.

$$T = \frac{8\pi(\lambda+1)}{\lambda[(2\lambda+1)!!]^2} \frac{1}{\hbar} \left(\frac{\omega}{c}\right)^{2\lambda+1} B(E\lambda; I_f \rightarrow I_i)$$

where the reduced transition probability $B(E\lambda; I_f \rightarrow I_i)$ for the decay is related by

$$B(E\lambda; I_f \rightarrow I_i) = \frac{2I_i + 1}{2I_f + 1} B(E\lambda; I_i \rightarrow I_f)$$

to the reduced transition probability $B(E\lambda; I_i \rightarrow I_f)$ for the excitation cross section; T is the probability per unit time for the transition, or $\frac{1}{\tau}$; $\omega = \Delta E/\hbar$, where ΔE is the transition energy. The data for plutonium-237 is as follows:⁵⁴

$$\Delta E = 145 \text{ keV}$$

$$t_{1/2} = 0.18 \text{ sec}$$

$$\text{Conversion coefficient} = 55$$

Thus,

$$T = 5.76 \times 10^{59} \Delta E^7 B(E\lambda; I_i \rightarrow I_f) \frac{2I_i + 1}{2I_f + 1}$$

And $B(E\lambda) = 5.11 \times 10^{-4}$. Substituting this value for $B(E\lambda)$ in the expression for $\sigma(E\lambda)$, we get

$$\sigma(E\lambda) = 9.298 \times 10^2 \left(1 + \frac{1}{235}\right)^{-4} \left(\frac{1}{235}\right)^4 E^{(3-2)} (E - \Delta E')^{(3-1)} \times (5.11 \times 10^{-4}) (3.8 \times 10^{-2})$$

If $\Delta E' \ll E$, then

$$\sigma(E\lambda) = 6.02 \times 10^{-12} E^3 \text{ barns}$$

The choice of E , the energy of the bombarding proton, is not clear-cut. Unfortunately, we cannot appeal to experiment--we have no direct access to hot interstellar gas or stellar envelopes. The flux of protons in near space is the only measurement that has been made, and we must assume that this is typical of the solar system over the past 10^9 years. The energy spectrum of these protons below 50 MeV is not certain, due to solar flare activity, but there are fewer particles in this energy range than in the higher energy portion of the spectrum. Above 50 MeV the number of particles varies as the -2.6 power of the energy, with a total flux of $1000 \text{ protons/m}^2\text{-ster-sec}$, $\pm 30\%$.⁵⁵

A reasonable approximation is to take the energy of the bombarding protons as 50 MeV, in which case

$$\sigma(E\lambda) = (6.02 \times 10^{-12})(1.25 \times 10^5) = 7.52 \times 10^{-7} \text{ barns}$$

The equilibrium ratio of isomeric state to ground state in such a proton flux is calculated as follows.

$$\text{Let the number of ground state uranium atoms per cm}^3 = N_0$$

$$\text{the proton flux} = n$$

$$\text{the number of isomeric uranium atoms per cm}^3 = N$$

The reaction rate of isomer formation is $N_0 n \sigma(E\lambda)$. The number of isomeric uranium atoms decaying to the ground state is $N \lambda_{U235m}$. Under equilibrium conditions,

$$N_0 n \sigma(E\lambda) = N \lambda_{U235m}$$

and

$$\frac{N}{N_0} = \frac{n \sigma(E\lambda)}{\lambda_{U235m}} = \frac{(1.2)(7.52 \times 10^{-31})}{4.44 \times 10^{-4}} = 2.03 \times 10^{-27}$$

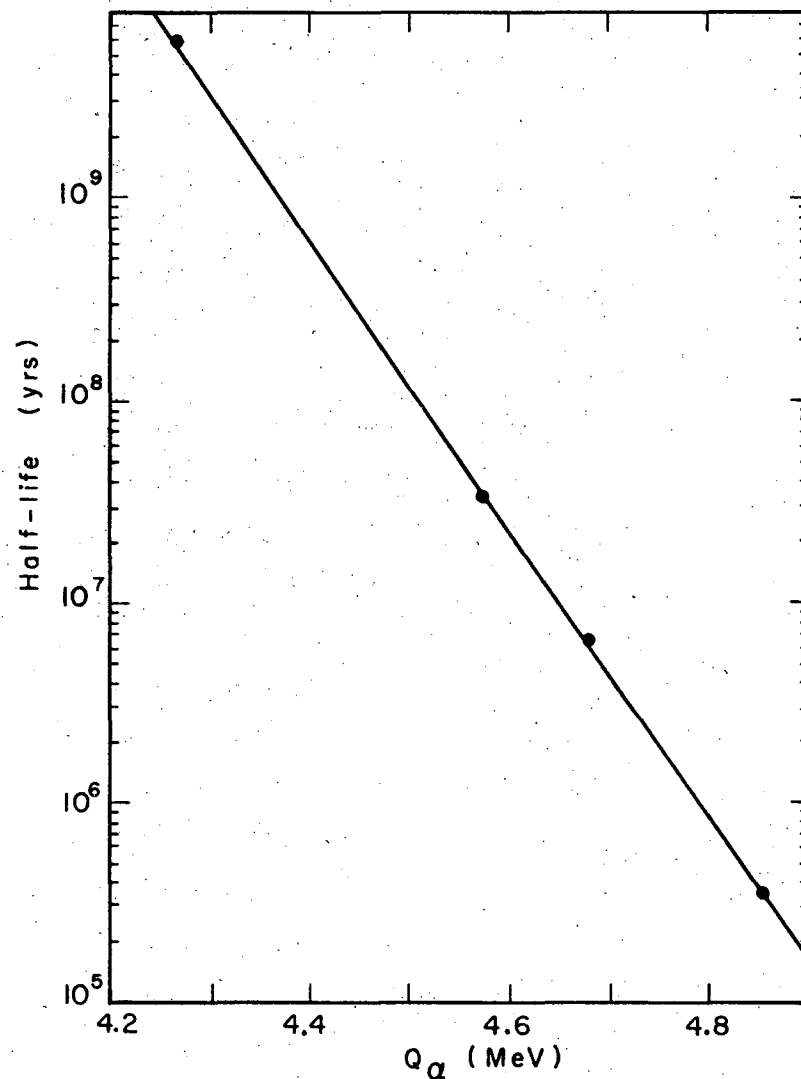
This ratio is exceedingly small, indicating that virtually no excitation of the isomer occurs in regions of space typified by our solar system. Nevertheless one cannot preclude the possibility of much larger proton fluxes in stellar envelopes operating over millions of year to produce a significant excitation of the isomer. Unless the half life for alpha decay of the isomer is very much shorter than that of the ground state, however, there will be no decrease in the ratio, $^{235}\text{U}/^{238}\text{U}$, even with proton fluxes several orders of magnitude greater than those observed.

C. Calculation of the Half Life for Alpha Decay of ^{235m}U

The calculation of the half life for alpha decay of the isomeric state is straightforward. Alpha transition rates exhibit an extremely sensitive exponential dependence on decay energy. A plot of the log of the half life vs. the decay energy for ground state to ground state transitions of even-even nuclei shows nearly straight line behavior for a given element. If the data from odd-N nuclei are placed on such a plot they will nearly always lie above their respective elemental lines (longer half lives). These transitions are said to be hindered. A hindrance factor may be defined for these nuclei as the ratio by which their half lives differ from a line interpolated between the nearest even-N isotopes. In these cases the orbital of the unpaired nucleon in

the parent and those of the excited states in the daughter nucleus are of utmost importance in determining the decay rate. Decays in which the orbital of the unpaired nucleon remains unchanged have low hindrance factors.

A plot of the unhindered half lives vs. Q_α (alpha particle energy plus recoil energy) for the uranium isotopes is shown in Fig. 28. The half lives are calculated using an equation due to Preston involving the nuclear radius and half lives of neighboring even-even nuclei.⁵⁶ This graph may be used to determine the unhindered partial half lives of the alpha groups of uranium-235m decaying to various states in thorium-231. To calculate the actual alpha half life of the isomer, the unhindered partial half lives for each alpha group must be multiplied by the hindrance factor for that group. Since these are unknown, they must be estimated. The isomeric state has been given the Nilsson assignment $(\Omega\pi I N_n A) 1/2 + 1/2 631$. As we have seen, the unpaired neutron in the ground state of plutonium-239 has exactly the same configuration. It would be expected that the alpha decay of the isomeric state of uranium-235 would exhibit very nearly the same hindrance factors as plutonium-239. This effect can be demonstrated in the case of plutonium-241 and curium-243, whose ground states are both $5/2 + 5/2 (622)$. The hindrance factors of their alpha groups are shown in Fig. 29.⁵⁷ Similar correlations of hindrance factors may be observed in several other pairs of nuclei with the same ground state configurations. Thus it appears that the use of plutonium-239 hindrance factors with the unhindered half lives for the alpha particle groups of uranium-235m obtained from Fig. 28 is a valid approach for determining the alpha half life of uranium-235m. Figure 30 shows the calculations.



XBL718-4067

Fig. 28. Unhindered half life vs. Q_α for the isotopes of uranium.

Ground states:

^{241}Pu : 5/2+, 5/2, (6,2,2)

^{243}Cm : 5/2+, 5/2, (6,2,2)

Spin state in daughter nucleus	^{241}Pu	Hindrance Factors ^{243}Cm
1/2+, 1/2 (6,3,1)	1.79×10^3	3.09×10^3
3/2	5.33×10^2	5.65×10^2
5/2	7.43×10^2	1.33×10^3
7/2	1.67×10^2	2.15×10^2
5/2+, 5/2 (6,2,2)	6.86×10^{-1}	1.43×10^0
7/2	2.33×10^0	5.22×10^0
9/2	9.78×10^0	1.82×10^1

Fig. 29. Comparison of ^{241}Pu and ^{243}Cm hindrance factors.

Levels in thorium-231	E(MeV)	unhindered $t_{1/2}(y)$	H.F. for Pu-239	Estimated partial λ
spin energy(keV)	$(Q_\alpha - E_{\text{Th}})$	(est. from Fig. 29)	decay to state	for alpha group (yrs^{-1})
5/2 327	4.354	1.3×10^9	8.89	$\frac{0.693}{(8.89)(1.3 \times 10^9)} = 6.0 \times 10^{-11}$
3/2 288	4.393	7.0×10^8	11.9	$\frac{0.693}{(11.9)(7.0 \times 10^8)} = 8.2 \times 10^{-11}$
1/2+, 1/2 631	275	5.7×10^8	2.94	$\frac{0.693}{(2.94)(5.7 \times 10^8)} = 4.2 \times 10^{-10}$
9/2 240	4.441	3.2×10^8	75.4	$\frac{0.693}{(75.4)(3.2 \times 10^8)} = 2.9 \times 10^{-11}$
7/2 169	4.512	1.0×10^8	285	$\frac{0.693}{(285)(1.0 \times 10^8)} = 2.4 \times 10^{-11}$
5/2 114	4.567	4.0×10^7	69.1	$\frac{0.693}{(69.1)(4.0 \times 10^7)} = 2.5 \times 10^{-10}$
3/2+, 3/2 631	75	2.15×10^7	670	$\frac{0.693}{(670)(2.15 \times 10^7)} = 4.8 \times 10^{-11}$
9/2 234			?	
7/2 204			?	
5/2-, 5/2 752	185		?	

(continued)

Levels in thorium-231 spin	energy(kev)	E(MeV) ($Q_\alpha - E_{Th}$)	unhindered $t_{1/2}(y)$ (est. from Fig. 29)	H.F. for Pu-239 decay to state	Estimated partial λ for alpha group (yrs^{-1})
9/2	97	4.584	3.1×10^7	632	$\frac{0.693}{(632)(3.1 \times 10^7)} = 3.5 \times 10^{-11}$
7/2	42	4.639	1.25×10^7	1170	$\frac{0.693}{(1170)(1.25 \times 10^7)} = 4.7 \times 10^{-11}$
5/2+, 5/2	633	0	6.4×10^6	589	$\frac{0.693}{(589)(6.4 \times 10^6)} = 1.8 \times 10^{-10}$

$$\lambda_{total} = 8.5 \times 10^{-10} + 32.5 \times 10^{-11} = 11.8 \times 10^{-10}$$

$$\text{half life of uranium-235m} = \frac{0.693}{11.8 \times 10^{-10}} = 5.9 \times 10^8 \text{ years}$$

Fig. 30. Calculation of alpha decay half life of uranium-235m. (Refs. 58 and 59).

The partial decay constants for the alpha groups are added to obtain the total decay constant, $1.18 \times 10^{-9} \text{ year}^{-1}$. The total half life for alpha decay is thus 5.9×10^8 years.

It should be noted that this value depends very strongly on the energies of the levels in thorium-231. If any of the levels are lowered by interaction due to Coriolis forces with a lower energy state, the alpha decay half life for uranium-235m would be smaller accordingly. A large effect would be unlikely, however, since the lowest thorium-231 levels, shown in Fig. 30, are all derived from different single particle levels, and there is probably little Coriolis mixing.

D. Cosmological Consequences

The value for the alpha decay half life of uranium-235m, 5.9×10^8 years, is quite close to that of the ground state, 7.1×10^8 years. This fact combined with the very low probability of Coulomb excitation in space renders it extremely unlikely that there has been any significant change in the ratio $^{235}\text{U}/^{238}\text{U}$ between the time of element synthesis and incorporation of the material into the solar system.

VII. SUMMARY AND CONCLUSIONS

The decay energy of the isomeric state of uranium-235 has been determined by means of a specially-designed micro-calorimeter capable of detecting 10^{-9} watt. This instrument is a Wheatstone bridge calorimeter in which two arms of the bridge are matched thermistors. One thermistor serves as a sample-holder; the other is a reference resistance. As the twenty-six-minute half life activity of the isomer decays, the temperature and, therefore, the resistance of the sample-holding thermistor change, creating an imbalance in the bridge, which was measured. The calorimeter was calibrated by an accurately measured radio frequency signal.

Uranium-235m is formed by the alpha decay of plutonium-239, so the sample of uranium-235m was obtained by a diethyl ether extraction from a plutonium-239 stock solution which was maintained in the Pu(III) oxidation state by ferrous sulfamate. Zinc nitrate was the salting-out agent. After evaporation to less than 1/2 cc, the sample was run through an anion exchange column to separate the uranium from inorganic mass, and it was then deposited on the thermistor. The curve obtained from the calorimeter was analyzed in a manner similar to that used in analysis of compound radioactive decay curves. The total decay energy of uranium-235m was found to be 572 ± 33 eV.

The nuclear properties of the isomeric state are of interest since it represents a possible loss mechanism of uranium-235 in space, which would affect the calculation of the age of the galaxy by Hoyle and others, using the ratio uranium-235/uranium-238. Hence, the half life for alpha decay of the isomeric state was calculated, using the unhindered half lives of the uranium isotopes to obtain an unhindered half life for

the isomer. This value was then corrected by applying the hindrance factors for the alpha decay of plutonium-239, which has the same intrinsic spin state as uranium-235m. The half life for alpha decay of the isomeric state was calculated to be 5.9×10^8 years, nearly equal to that of the ground state.

Using the expression for the probability of Coulomb excitation derived by Alder, Bohr, Huus, Mottelson, and Winther, it was found that the Coulomb excitation of uranium-235m by protons in regions of space typified by our solar system is negligible.

It was therefore concluded that the existence of the isomeric state poses no problem in the determination of the age of the galaxy.

ACKNOWLEDGMENTS

I wish to thank:

Dr. I. Perlman, who first suggested the calorimetry experiment and served as my faculty advisor.

Herman P. Robinson, for invaluable aid in the design, construction and trouble-shooting of the calorimeter.

Dr. Frank Asaro, for helpful discussions during the course of the work and especially valuable aid with the alpha half-life calculation.

Mrs. Helen V. Michel, for the bismuth-212 sample.

Dr. Richard Diamond, who aided in the Coulomb excitation calculation and generously permitted the use of his laboratory space for the experiment.

Dr. R. S. Newbury, who performed the mass analysis of the plutonium stock solution.

Mr. Jerry Bucher helped immeasurably in the performance of the solvent extraction portion of the procedure and in addition supplied cheering conversation about snow conditions in the Sierras and other vital topics.

Mrs. Elinor Potter furnished unstinting aid in all phases of the work.

The late Mr. George Driscoll of Safety Services was my indispensable right hand man and morale booster.

Dr. G. H. Spremulli, Dr. F. R. Griffith, and Dr. J. R. Murray, of Elmira College, Elmira, New York, have provided continuing warm encouragement and interest in the years since my graduation.

My parents, Mr. and Mrs. Alfred Bailey, have been my staunchest supporters.

Finally, I thank my son, Timothy, whose impending arrival served as the impetus for the completion of the experiments; and, especially, my husband, Vaughn, whose unfailing aid, encouragement and understanding were the major factors in the success of the work.

REFERENCES

1. J. R. Huizenga, D. W. Engelkemeir, and F. Tomkins, *Bull. Am. Phys. Soc. II* 2, 198 (1957).
2. K. N. Shliagin, *Trans. Soviet Phys. JETP* 3, 663 (1956).
3. F. Asaro and I. Perlman, *Phys. Rev.* 107, 318 (1957).
4. J. R. Huizenga, C. L. Rao, and D. W. Engelkemeir, *Phys. Rev.* 107, 319 (1957).
5. M. C. Michel, F. Asaro, and I. Perlman, *Am. Phys. Soc. Bull. II* 2, 394 (1957).
6. M. S. Freedman, F. T. Porter, F. Wagner, and P. P. Day, *Phys. Rev.* 108, 836 (1957).
7. H. Mazaki and S. Shimizu, *Phys. Letters* 10/10/66.
8. N. de Mevergnies, to be published.
9. J. N. Shive, *Semiconductor Devices*, (D. Van Nostrand and Co., Princeton, 1959), p. 15.
10. E. Peligot, *Ann. Chim. Phys.* (3) 5, 1 (1842).
11. E. K. Hyde, *Proceedings of the International Conference on the Peaceful Uses of Atomic Energy*, Vol. 7, United Nations, New York, 1956, p. 281.
12. A. W. Gardner, H. A. C. McKay, and D. T. Warren, *Trans. Faraday Soc.* 48, 997 (1952).
13. L. I. Katzin and J. C. Sullivan, *J. Phys. Chem.* 55, 346 (1951).
14. N. H. Furman, R. J. Mundy, and G. H. Morrison, USAEC Rep. AECD-2938.
15. *Ibid.*
16. I. L. Jenkins and H. A. C. McKay, *Trans. Faraday Soc.* 50, 109 (1954).
17. V. M. Vdovenko and T. V. Kovaleva, *J. Inorg. Chem. USSR* 2, No. 7, 368 (1957).

18. J. E. Grindler, *The Radiochemistry of Uranium*, N.A.S., Office of Technical Services, Department of Commerce, Washington, D. C. (1962).
19. L. I. Katzin, D. M. Simon, and J. R. Ferraro, *J. Am. Chem. Soc.* 74, 1191 (1952).
20. E. K. Hyde, *op. cit.*, p. 728.
21. A. A. Kuznetsova, O. Ya. Samilov, and V. I. Tikhomirov, *Radiokhimiya* 3, No. 1, 10-13 (1961).
22. N. H. Furman, R. J. Mundy, and G. H. Morrison, *op. cit.*, p. 18.
23. J. C. Hindman, Report CN-1702, June 1, 1944.
24. A. Brunstad, *HW 51655*, July, 1957.
25. W. Latimer, *Oxidation Potentials*, (Prentice Hall, Englewood Cliffs, New Jersey, 1952), p. 93.
26. D. A. Costanzo and R. E. Biggers, *ORNL - TM - 585*, July, 1963.
27. A. Brunstad, *HW 54203*, December, 1957.
28. G. Coleman, *Radiochemistry of Plutonium*, NAS - NS 3058, 1965.
29. D. W. Ockenden and G. A. Welch, *J. Chem. Soc.* 1956, pp. 3358-63.
30. F. J. Miner, Dow Chemical Co. Rocky Flats Plant, *RFP - 357*, January, 1964.
31. D. A. Costanzo and R. E. Biggers, *op. cit.*
32. C. K. McLane, *CN - 2689*, March, 1945.
33. F. J. Miner, *op. cit.*
34. D. A. Costanzo and R. E. Biggers, *op. cit.*
35. S. Peterson and R. G. Symer, *Chemistry in Nuclear Technology*, (Addison-Wesley, Reading, Massachusetts, 1963), p. 169.
36. R. Feinstein, U. S. Patent #3003002.
37. B. A. Adams and E. L. Holmes, *J. Soc. Chem. Ind. (London)* 54, 1T (1935).

38. Foreman, McGowan, and Smith, J. Chem. Soc. 1959, 738.
39. J. L. Ryan, J. Phys. Chem. 65, 1099 (1961).
40. D. C. Whitney, Ph.D. Thesis, University of California, Berkeley, 1962.
41. F. Nelson, T. Murase, and K. A. Kraus, J. Chromatog. 13, 503 (1964).
42. Ibid.
43. Michele Veisiere, and Bernard Tremillon, Bull. Soc. Chim. France 7, 2099-2103 (July, 1965).
44. Kraus, Nelson, and Moore, J. Am. Chem. Soc. 77, 3972 (1955).
45. Boase and Foreman, Talanta 8, 187 (1960).
46. Korkisch, Farag, and Hecht, Z. Anal. Chem. 161, 92 (1958).
47. E. M. Burbidge, G. R. Burbidge, W. A. Fowler, and F. Hoyle, Rev. Mod. Phys. 29, 547 (1957).
48. H. Suess and H. Urey, Rev. Mod. Phys. 28, 53 (1956).
49. W. A. Fowler and F. Hoyle, Ann. Phys. 10, 280 (1960).
50. W. A. Fowler, Proc. Nat. Acad. Sci. 52, 524 (1964).
51. D. C. Clayton, Science 143, 1281 (1964).
52. R. H. Dicke, Astrophys. J. 155, 123 (1969).
53. R. Alder, A. Bohr, T. Huus, B. Mottelson, and A. Winther, Rev. Mod. Phys. 28, 432 (1956).
54. F. S. Stephens, Jr., and F. Asaro, unpublished data.
55. P. Mayer, Ann. Rev. Astron. & Astrophys., 1970.
56. M. A. Preson, Phys. Rev. 71, 865 (1947).
57. H. V. Michel, Lawrence Radiation Laboratory Report UCRL-9229, (1960).
58. John Erskine, unpublished data.
59. Elze, Egidy, and Huizenga, Nucl. Phys. A128, 564 (1969).

LEGAL NOTICE

This report was prepared as an account of work sponsored by the United States Government. Neither the United States nor the United States Atomic Energy Commission, nor any of their employees, nor any of their contractors, subcontractors, or their employees, makes any warranty, express or implied, or assumes any legal liability or responsibility for the accuracy, completeness or usefulness of any information, apparatus, product or process disclosed, or represents that its use would not infringe privately owned rights.

TECHNICAL INFORMATION DIVISION
LAWRENCE BERKELEY LABORATORY
UNIVERSITY OF CALIFORNIA
BERKELEY, CALIFORNIA 94720